Supporting Information

Boronic acid and diol-containing polymers: how to choose the correct couple to form "strong" hydrogels at neutral pH.

Tamiris Figueiredo,[a] Vanina Cosenza,[a] Yu Ogawa,[a] Isabelle Jeacomine,[a] Alicia Vallet,[b] Sonia Ortega,[a] Raphael Michel,[a] Johan D. M. Olsson,[d] Thibaud Gerfaud,[c] Jean-Guy Boiteau,[c] Jing Jing,[c] Craig Harris,[c] Rachel Auzély-Velty[a]*

[a] Univ. Grenoble Alpes, Centre de Recherches sur les Macromolécules Végétales (CERMAV)-CNRS, 601, rue de la Chimie, BP 53, 38041 Grenoble Cedex 9 (France).

[b] Univ. Grenoble Alpes, CEA, CNRS, Institut de Biologie Structurale, 71 avenue des Martyrs, 38044 Grenoble Cedex 9 (France)

[c] Galderma/Nestlé Skin Health R&D, 2400 Route de Colles, 06410 Biot (France)

[d] Galderma/Nestlé Skin Health R&D, Seminariegatan 21, SE-752 28 Uppsala (Sweden)

Table of Contents

1. Materials and characterization methods

Materials. Sodium hyaluronate (HA) possessing a weight average molar mass (M_w) of 100 kg/mol was supplied by Lifecore Biomedical (USA). The molar mass distribution and the weight-average molar mass of this sample were determined by size exclusion chromatography using a Waters GPC Alliance chromatograph (USA) equipped with a differential refractometer and a light scattering detector (MALLS) from Wyatt (USA); the solution was injected at a concentration of 1×10^{-3} g/mL in 0.1 M $NaNO_3$, at a flow rate of 0.5 mL/min and at a column temperature of 30 °C. The dispersity ($Đ$) of the sample is $M_w/M_n \approx 1.5$-2. The overlap concentration C^* for this HA sample in buffer at 25 °C is around 3 g/L. This value was derived from the intrinsic viscosity assuming that $C^*[\eta]$ is about unity.[1] HA samples with lower M_w (5 or 10 kg/mol), purchased from the same supplier, were used to synthesize HA derivatives for NMR studies (thermodynamics, kinetics and elucidation of the structure of boronic acid complexes). This low M_w HA sample was used to circumvent limitations due to the high viscosity of concentrated solutions of high M_w HA. 5-amino-2-(hydroxymethyl)phenylboronic acid hydrochloride (ABOR, 6-aminobenzoboroxole) and Boc-1-amino-3,6-dioxa-8-octanamine (Boc-DOOA) were purchased from Combi-Blocks and Iris Biotech, respectively. 1-Amino-1-deoxy-D-fructose hydrochloride (fructosamine) and D-gluconolactone were supplied by Carbosynth. 3-Aminophenylboronic acid hemisulfate salt (APBA), 4-(4,6-dimethoxy-1,3,5-triazin-2-yl)-4-methylmorpholinium chloride (DMTMM), D-maltose, 1-thio-β-D-glucose sodium salt(thioglucose), 4-pentenoic anhydride, O-(carboxymethyl)hydroxylamine hemihydrochloride, cysta-mine dihydrochloride, N,N'-diisopropylcarbodiimide (DIC), 1-hydroxybenzotriazole (HOBT), tris(2-carboxyethyl)phosphine hydrochloride (TCEP), trifluoroacetic acid (TFA), picrylsulfonic acid solution (TNBS), 4-(2-hydroxyethyl)piperazine-1-ethanesulfonic acid (HEPES), phosphate buffered saline (PBS) and other chemicals were purchased from Sigma-Aldrich-Fluka and were used with-out further purification. A ^{13}C labeled maltose (maltose-$^{13}C_{12}$ monohydrate) was supplied by Cambridge Isotope Laboratoires and a ^{13}C labeled D-fructose was purchased from Carbosynth.

Methods.

NMR spectroscopy. ^1H, ^{13}C and 2-D INADEQUATE NMR spectra were recorded at 25 °C or 80 °C using a Bruker AVANCE III HD spectrometer operating at 400.13 MHz (^1H) and at 100.61 MHz (^{13}C). ^1H NMR spectra were recorded by applying a 90° tip angle for the excitation pulse, and a 10 s recycle delay for accurate integration of the proton signals. ^{13}C NMR spectra were recorded by applying a 90° tip angle for the excitation pulse and a 2 s recycle delay. 2D INADEQUATE experiments were per-formed using the pulse sequence inadphsp given by Bruker. For each experiment, 256 transients were acquired for each of the 128 increments in F1. The recycle delay was set to 3 s. The spectral width was set to 20161 Hz (number of data points = 8192). The data were processed with shifted sine bell weighting and zero filling to form a 8192 x 1024 matrix prior to Fourier transform. ^{13}C-edited HSQC experiments using the HA derivative modified with ^{13}C labeled maltose were recorded on a Bruker AVANCE III HD operating at 950.23 MHz (^1H) and at 238.94 MHz (^{13}C) equipped with a cryogenic probe. Deuterium oxide (D_2O) was obtained from Eurisotop (Saint-Aubin, France). Chemical shifts (δ in ppm) are given relative to external tetramethylsilane (TMS = 0 ppm) and calibration was performed using the signal of the residual protons of the solvent as a secondary reference. All NMR spectra were analyzed with Topspin 3.1 (or 3.5) software from Bruker AXS.

Rheology. Oscillatory shear experiments were performed with a cone-plate rheometer (AR2000EX from TA Instruments). All the dynamic rheological data were checked as a function of strain amplitude to ensure that the measurements were performed in the linear viscoelastic region. No frequency data beyond 10 Hz are presented because inertial artefacts (raw phase angle > 150°) were observed at frequencies higher than 10 Hz.[2,3] The cone used for viscoelastic samples has a diameter of 2 cm and an angle of 4°, whereas viscous solutions were analyzed using a cone of 6 cm of diameter and an angle of 1°. To prevent water evaporation, the measuring system was surrounded with a low-viscosity silicon oil (50 mPa.s) carefully added to the edges of the cone.

Determination of K_a by ITC. Calorimetric titration experiments were carried out on a Microcal VP-ITC titration microcalorimeter (Northampton, U.S.A.). All titrations were performed using solutions of APBA (ABOR) and free saccharides (D-fructose, maltose-COOH and gluconamide) solubilized in

0.01 M PBS, with pH adjusted to 7.4 (± 0.1) using a pH-meter, by carefully adding 1 M NaOH when necessary. The reaction cell (V = 1.4478 mL) contained a solution of “molecule 2” (Table S1). A series of 28 injections of 5 or 10 µL of a solution of “molecule 1” was made from a computer-controlled 300 µL microsyringe at an interval of 400 s into the solution contained in the reaction cell, while stirring at 300 rpm at 25°C. The raw experimental data were reported as the amount of heat produced after each injection of boronic acid as a function of time. The amount of heat produced per injection was determined by integration of the area under individual peaks by the instrument software, after taking into account heat of dilution.The data were analyzed using the one set of site fitting model (Origin 7.0 software package). Table S1 summarizes the experimental conditions used for the ITC measurements.

Table S1. Experimental conditions of the calorimetric titrations.

Entry	Molecule 1 in syringe	[Molecule 1] (mM)	Molecule 2 in cell	[Molecule 2] (mM)
1	Free D-fructose	130	APBA	3.7
2	Free D-fructose	75	ABOR	2
3	APBA	15	Free maltose-COOH	0.5
4	ABOR	35	Free maltose-COOH	1
5	APBA	20	Free gluconamide	1
6	ABOR	35	Free gluconamide	1

Computational analysis. Four possible tricovalent PBA/maltose complexes (Figure 5, main text), formed between the open glucose unit of the maltose derivative and PBA, have been studied: two bridged bicyclic compounds formed by 5- and 6-membered rings (complexes **2** and **4**) and two bridged bicyclic compounds formed by 5- and 7-membered rings (complexes **1** and **3**). For a better representation of the maltose derivative which is grafted to HA, C1 of the open glucose unit was replaced by a vinyl group. First, force field molecular dynamics (MD) simulations were carried out on the complexes for screening the different rotamers and rings conformations. The MD simulations were performed in the GROMACAS software, ver. 2018,[4] with all-atom Gromos 54a7 force field.[5] All the MD simulations were performed in an NPT (constant number of atoms, pressure, and temperature) ensemble with velocity-rescale temperature coupling[6] and Berendsen pressure coupling algorithms[7] with temperature and pressure coupling con-stants of 0.2 ps and 2 ps, respectively. Each complex was placed in a box with dimensions with 5×5×5 nm^3 where single point charge (SPC) water molecules[8] are filled. The structure is then relaxed with energy minimization followed by MD simulation with slow heating from 0 K to 300 K in 2 ns. The system was then equilibrated for 8 ns at 300 K. The production run was performed for 10 ns at 300 K. From the above MD simulations, the feasible conformers and rotamers of the different complexes were selected and submitted to DFT calculations using Gaussian 09 (rev. D.01)[9] with standard termination options. Optimizations were performed with M062X[10] at 6-311+G(d,p) level and with SMD[11] in water. The functional was chosen for its proven performance in estimations of the relative energies of sugar conformers[12,13] and B-O bond length.[14] The SMD solvent simulation was chosen as it was shown to well reproduce the solvation effect.[12] For each DFT optimization, a frequency calculation was performed in order to verify that there is no negative frequency (i.e. confirm that it is a minimum) and to determine the absolute free energy of each rotamer at 298 K. For the complexes of PBA and an open glucose used to simulate the gluconamide derivative (with the C1 replaced by a vinyl group), ten different tricovalent possibilities have been studied: three bridged bicyclic compounds formed by two 5-membered rings and four bridged bicyclic compounds formed by 5- and 6-membered rings, one bridged bicyclic compound formed by two 6-membered rings and two bridged bicyclic compounds formed by 5- and 7-membered rings. In this case, only DFT calculation was performed for all possible rotamers of each complex, using the same condition described for the PBA/maltose derivative complexes. For complexation between the grafted fructose and BOR with the open boroxole ring, a 1-acetamido fructose derivative was used to represent the amide bond between the monosaccharide and HA. Only MD simulation was carried out in the same condition as described for PBA/maltose derivative complexes.

2. Modification of hyaluronic acid with glucose or maltose moieties by thiol-ene photochemistry

The syntheses of HA-maltose and HA-glucose were performed via thiol-ene coupling reactions between a maltose-thiol derivative and commercially available thioglucose, respectively, and HA possessing alkene groups (HA-pentenoate)[15] (Figure S1). The maltose-thiol was prepared from a carboxylic acid derivative of maltose (maltose-COOH, Figure S1b) as previously described.[16] During the coupling reactions with HA-pentenoate, the thiol-to-ene ratios were adjusted to obtain a DS of 0.1 to 0.15 for the HA derivatives. Successful grafting of the saccharides onto HA was confirmed by ^{1}H NMR spectroscopy which also allowed determination of the DS (Figure S2).

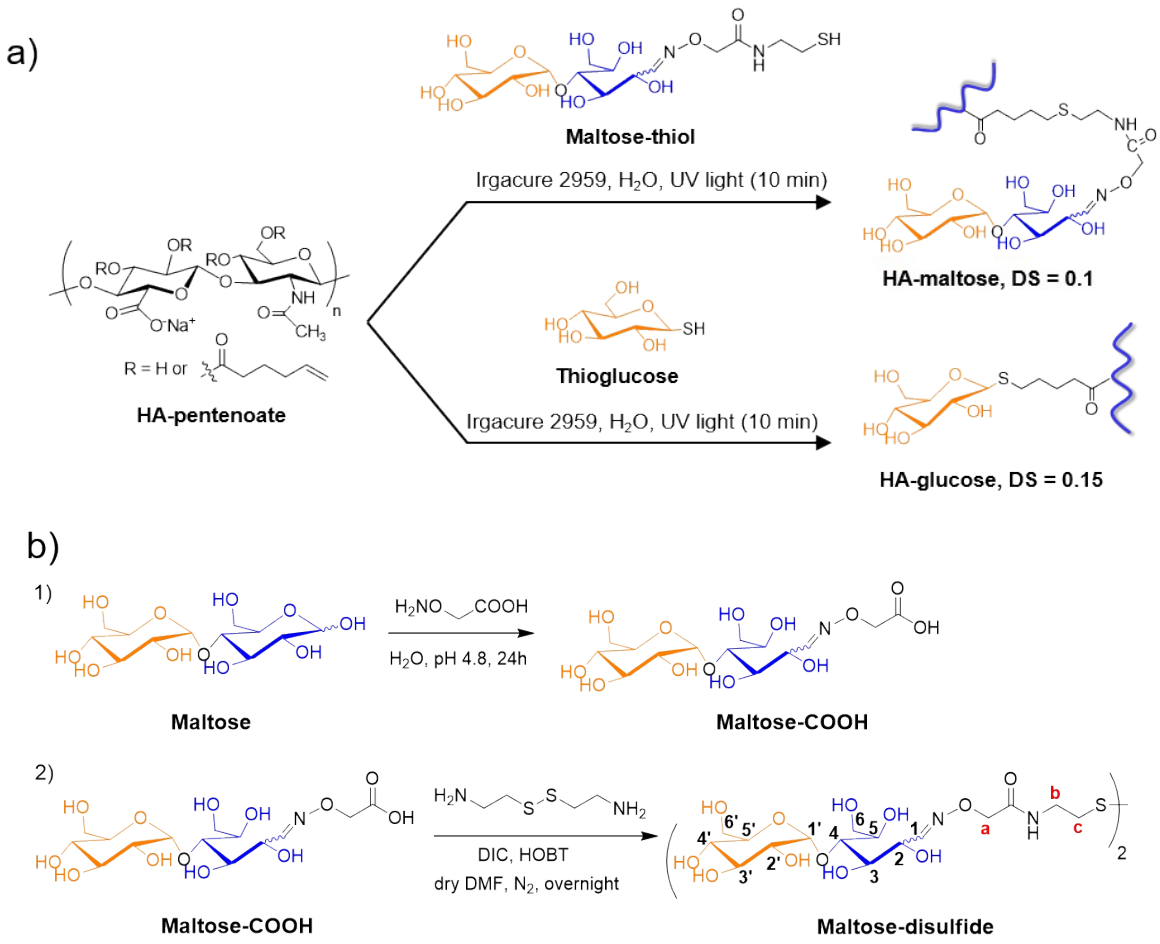

Figure S1. Synthetic scheme for the preparation of HA derivatives via thiol-ene coupling reaction (a), and synthesis of maltose-disulfide from a maltose-COOH derivative (b).

HA-maltose. The HA-maltose derivative was synthesized as previously reported.[16] In brief, this included a first step to prepare an unprotected carboxylic acid derivative of maltose (maltose-COOH) by reaction of D-maltose (0.5 g, 1.4 mmol) with *O*-(carboxymethyl)hydroxylamine (0.153 g, 1.4 mmol) in water at pH 4.8. Then, a maltose-disulfide derivative was obtained by reaction of maltose-COOH with cystamine dihydrochloride (0.157 g, 0.7 mmol) in dry DMF under nitrogen, using DIC (0.7 g, 5.57 mmol) and HOBT (0.38 g, 2.79 mmol). The synthesis of HA-maltose consisted in the reduction of the disulfide bond of maltose-disulfide (0.16 g, 1.69 mmol) with TCEP (0.062 g, 0.22 mmol), followed by the coupling reaction in ultrapure water of maltose-thiol with pentenoate-modified HA (0.25 g, 0.6 mmol), in the presence of the photoinitiator Irgacure 2959 (0.1 % w/v), at room temperature for ten minutes under UV light (λ = 365 nm, 20 mW/cm^2). Successful grafting of maltose-thiol onto HA was confirmed by ^{1}H NMR spectroscopy, which also allowed determination of a DS of 0.1 (Figure S2a, Table S2). ^{1}H NMR (400 MHz, D_2O, 25 °C) of maltose-disulfide (Figure S1b): δ_H (ppm) 7.54 and 6.89 (1H, H1), 5.33 (1H, H1'), 4.53 (2H, Ha), 3.95-3.40 (12H, H2-H6 and H2'-H6'), 2.60 (4H, Hb and Hc).

HA-glucose. The commercially available 1-thio-β-D-glucose (0.033 g, 0.15 mmol) was reacted with pentenoate-modified HA (0.1 g, 0.24 mmol) at room temperature for ten minutes under UV light in ultrapure water. ^{1}H NMR analysis of the product allowed determination of a DS of 0.15 of the HA-glucose derivative (Figure S2b, Table S2).

Table S2. Reaction conditions for the synthesis of HA-maltose and HA-glucose.

HA derivative	[SH]/[pentenoate]	DS[a]	Yield (%)
HA-maltose	1.6	0.1	88
HA-glucose	3.5	0.15	90

[a]DS by ^{1}H NMR (10 % of accuracy).

3. ^{1}H NMR spectra of HA derivatives synthesized by thiol-ene photochemistry

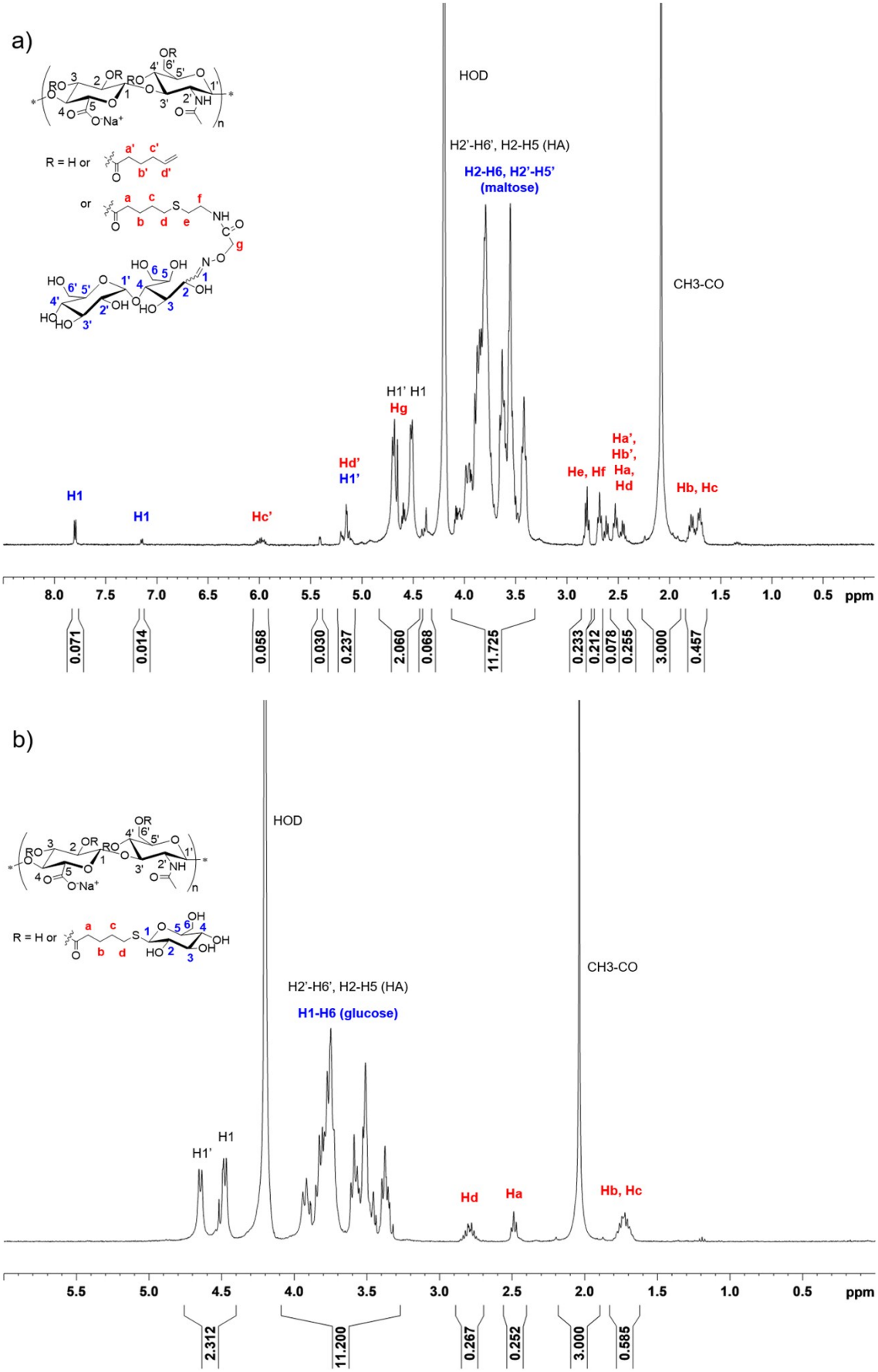

Figure S2. ^{1}H NMR spectra (400 MHz, D_2O, 6 mg.mL^{-1}, 80 °C) of HA-maltose (a) and HA-glucose (b).

4. Modification of hyaluronic acid with phenylboronic acid, benzoboroxole, fructose or gluconamide moieties by amide coupling reaction

The HA-PBA, HA-BOR, HA-fructose and HA-gluconamide derivatives were prepared by an amide coupling reaction carried out in aqueous solution between 3-aminophenylboronic acid (APBA), 6-amino-1-hydroxy-2,1-benzoxaborolane (6-aminobenzoboroxole, ABOR), 1-amino-1-deoxy-D-fructose (fructosamine) and a glucose derivative in the ring-opened form (1-amino-DOOA-gluconamide), respectively, and HA, using 4-(4,6-dimethoxy-1,3,5-triazin-2-yl)-4-methylmorpholinium chloride (DMTMM) as a coupling agent (Figure S3).[17] For the synthesis of the 1-amino-DOOA-gluconamide, D-gluconolactone was reacted with Boc-1-amino-3,6-dioxa-8-octanamine (Boc-DOOA) according to a previously reported procedure, affording Boc-1-amino-DOOA-gluconamide (Figure S3b).[18] The DS of the HA conjugates was controlled by the amount of amine-to-carboxylic acid. Using DMTMM/HA and amine/HA molar ratios of 1 and 0.15 to 0.2, respectively, we obtained HA derivatives with a DS of 0.1 to 0.15 from ^{1}H or ^{13}C NMR analysis (Figure S4-S6). In the case of HA-fructose and HA-gluconamide, the DS was also estimated from the reaction kinetics performed using 2,4,6-trinitrobenzene sulfonic acid (TNBS) to quantify the free primary amines in the reaction medium as a function of time (Figure S7).

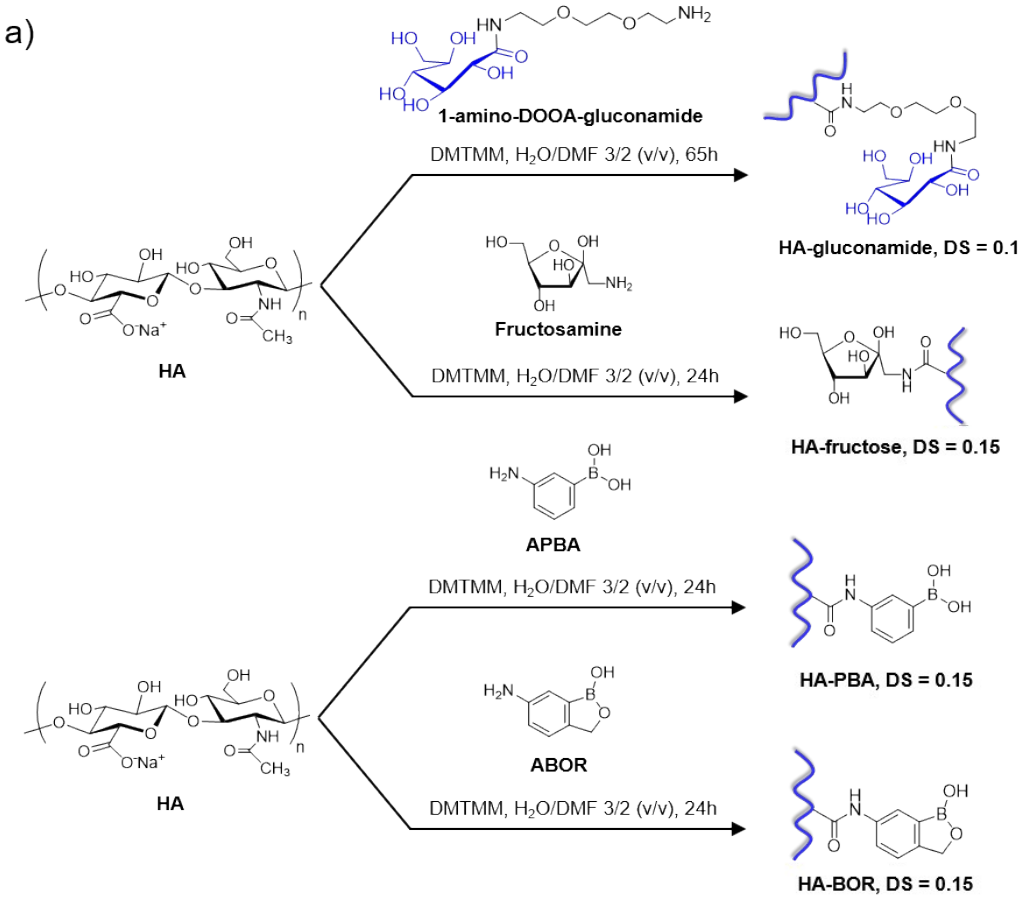

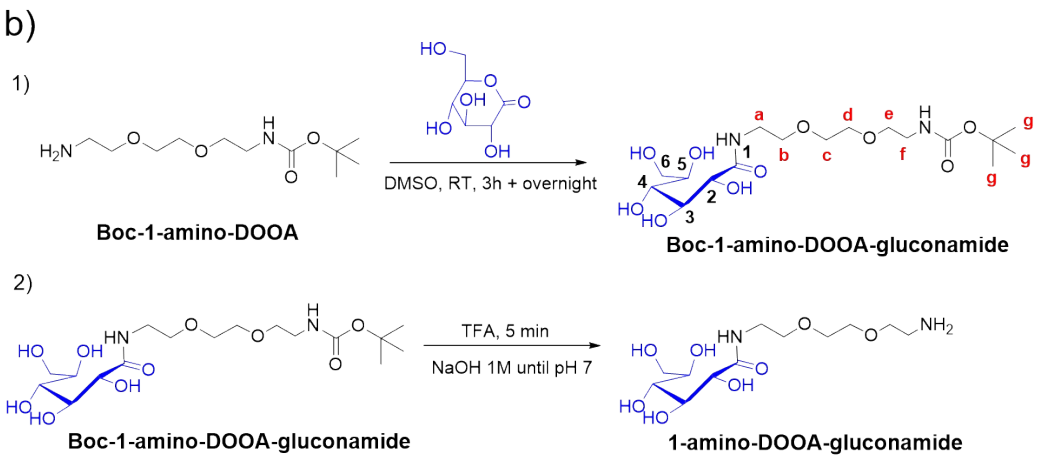

Figure S3. Synthetic scheme for the preparation of HA derivatives via amide coupling reaction (a), and synthesis of 1-amino-DOOA-gluconamide from a Boc-1-amino-DOOA-gluconamide derivative (b).

HA-gluconamide. To a solution of Boc-DOOA (0.113 g, 0.45 mmol) in DMF (25 mL), a solution of D-glucono-1,5-lactone (0.081 g, 0.45 mmol) in DMF (20 mL) was added dropwise for ~ 3 h. After stirring overnight at room temperature, the solvent was removed under reduced pressure and the resulting transparent syrup was dried under vaccum (60 mbars, 40 °C) to give a Boc-DOOA-gluconamide derivative (0.178 g, 92 %). The removal of the Boc protecting group was performed by acid treatment of Boc-DOOA-gluconamide (0.055 g, 0.13 mmol) in TFA (0.6 mL, 7.77 mmol) for 5 min at room temperature. The reaction medium was neutralized by adding 1 M NaOH dropwise (≈ 5 mL) at ~ 0 °C, and the solvent was removed under reduced pressure. The complete deprotection of the amine group yielding 1-amino-DOOA-gluconamide derivative was confirmed by ^{1}H NMR analysis. The HA-gluconamide derivative was then prepared by amide coupling. The reaction consisted in adding DMTMM (0.207 g, 0.75 mmol) to a solution of HA (0.3 g, 0.75 mmol) at a concentration of 3 g/L in a water/DMF (3/2, v/v) mixture. After 15 min of stirring at room temperature, 1-amino-DOOA-gluconamide (0.056 g, 0.17 mmol) was added and the pH was adjusted to 6.5 using 0.5 M aqueous NaOH. After stirring for 65 h at room temperature, the HA-gluconamide conjugate was purified by ultrafiltration using deionized water and the product was recovered by freeze-drying (Table S3). The DS of HA-gluconamide was found to be 0.1 from ^{13}C NMR analysis (Figure S5). It was also estimated from the reaction kinetics performed by quantifying the free primary amine in the reaction medium as a function of time (Figure S7). ^{1}H NMR (400 MHz, D_2O, 25 °C) of **Boc-1-amino-DOOA-gluconamide** (Figure S3b): δ_H (ppm) 4.35 (1H, H2), 4.15 (1H, H3), 3.88-3.72 (10H, H4-H6 and Hb-Hd), 3.65 (2H, He), 3.55 (2H, Ha), 3.32 (2H, Hf), 1.5 (9H, Hg).

HA-PBA, HA-BOR and HA-fructose. HA-PBA, HA-BOR and HA-fructose were synthesized by an amide coupling reaction from APBA, ABOR and fructosamine (containing free primary amine groups), respectively. To this end, APBA (0.022 g, 0.12 mmol) or ABOR (0.025 g, 0.135 mmol) or fructosamine (0.024 g, 0.112 mmol) was added to a water/DMF (3/2, v/v) mixture containing DMTMM (0.207 g, 0.75 mmol) and HA (0.3 g, 0.75 mmol) and the pH was adjusted to 6.5 using 0.5 M aqueous NaOH. After stirring for 24 h at room temperature, the different HA derivatives were purified by ultrafiltration using deionized water and the products were recovered by freeze-drying (Table S3). The DS of the HA derivatives were found to be 0.15 from ^{1}H and ^{13}C NMR analyses (Figure S4 and S6). The DS of HA-fructose was also estimated from the reaction kinetics using the TNBS method (Figure S7).

Table S3. Reaction conditions for the synthesis of HA-BOR, HA-PBA, HA-fructose and HA-gluconamide.

HA derivative	R-NH_2/HA molar ratio	DS	Coupling (%)	Yield (%)
HA-BOR	0.18	0.15[a]	83	86
HA-PBA	0.16	0.15[a]	100	98
HA-fructose	0.15	0.15[b]	100	96
HA-gluconamide	0.22	0.1[b,c]	50	73

[a]DS by ^{1}H NMR (10 % of accuracy).
[b]DS estimated from the reaction kinetics using TNBS.
[c]DS by ^{13}C NMR (20 % of accuracy).

5. ^{1}H NMR spectra of HA derivatives synthesized by amide coupling reaction

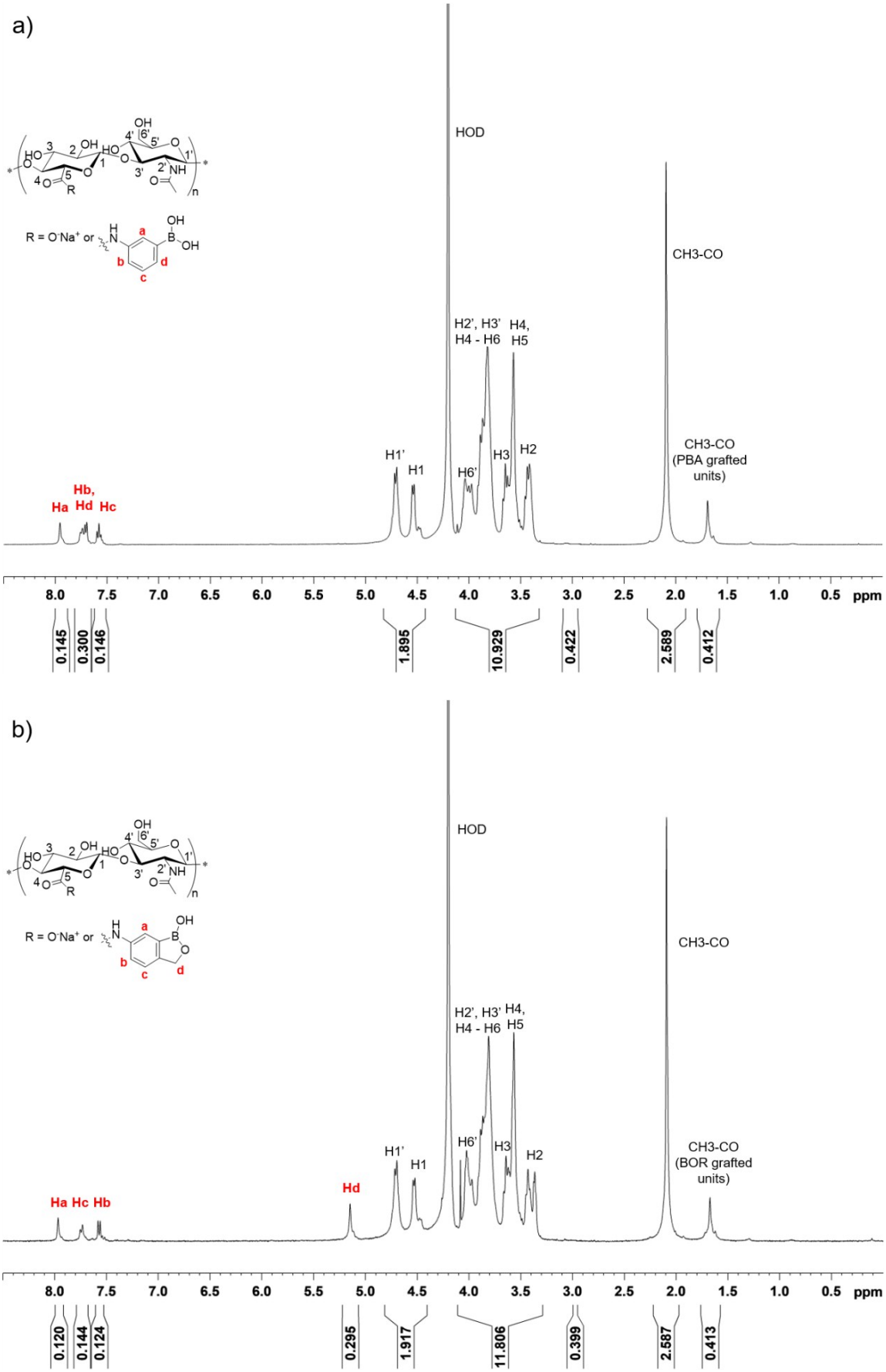

Figure S4. ^{1}H NMR spectra (400 MHz, D_2O, 6 mg.mL^{-1}, 80 °C) of HA-PBA (a) and HA-BOR (b).

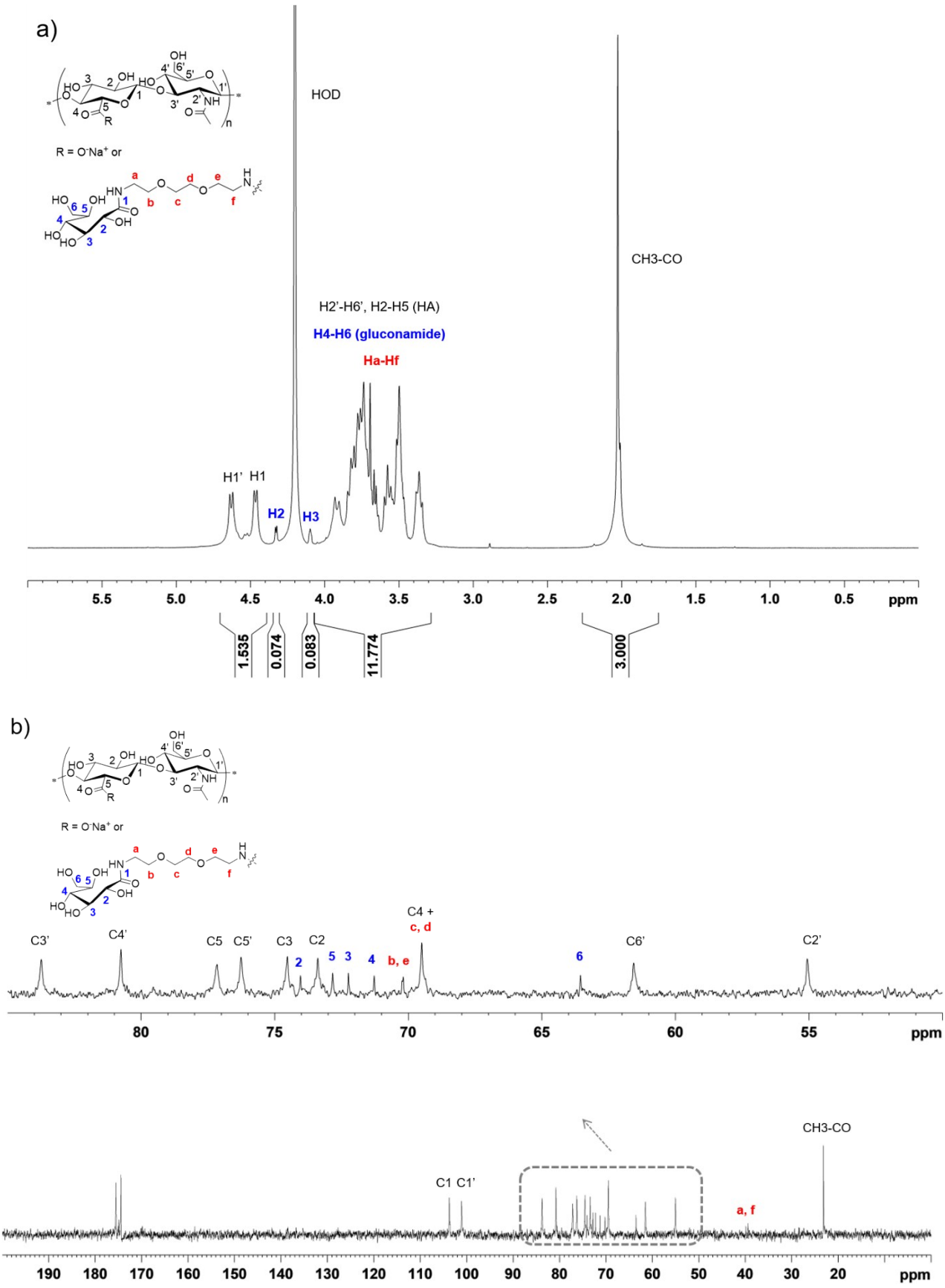

Figure S5. ^{1}H (a) and ^{13}C (b) NMR spectra (400 or 100 MHz, D_2O, 6 mg.mL^{-1}, 80 °C) of HA-gluconamide.

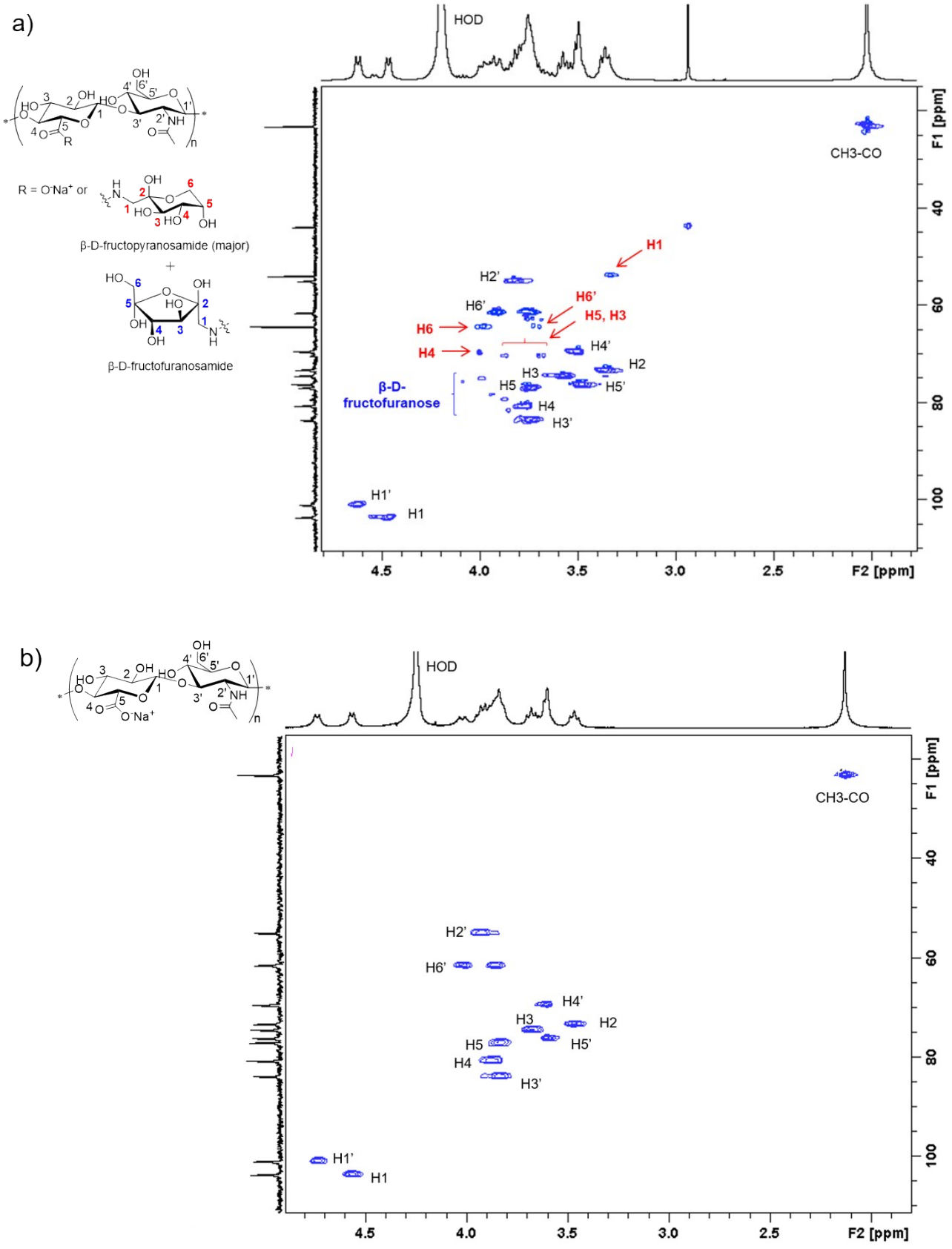

Figure S6. 2D HSQC NMR spectra (400 MHz, D_2O, 6 mg.mL^{-1}, 80 °C) of HA-fructose (a) compared to native HA (b). Of note, β-D-fructopyranose is the major tautomeric form observed for grafted fructose moieties, followed by the β-D-fructofuranose form.

6. Determination of the degree of substitution (DS) of HA-fructose (HA-gluconamide) from the kinetics of the amide coupling reaction

As the superposition of ^{1}H signals of HA and grafted fructose (or gluconamide) moieties precluded determination of the DS of HA-fructose (HA-gluconamide) by ^{1}H NMR, their DS were estimated from the kinetics of their syntheses, by quantifying the free primary amines in the reaction medium as a function of time. This was based on the reaction of fructosamine (or 1-amino-DOOA-gluconamide) with 2,4,6-Trinitrobenzene Sulfonic Acid (TNBS), which gives an orange-colored final product (trinitrophenylamine) that absorbs in the UV region, at around 340 nm (Scheme 1).[19]

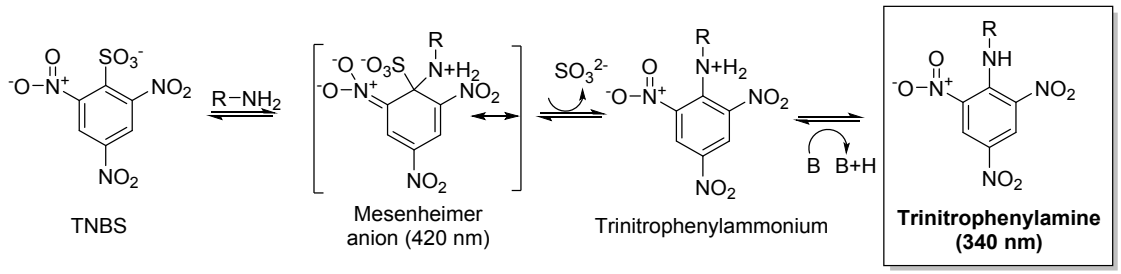

Scheme 1. Trinitrophenylation of primary amines with TNBS.

Procedure for the reaction kinetics by quantifying primary amines with TNBS

The methodology to quantify primary amines with TNBS was adapted from a procedure previously described.[20] Standard curves of primary amines (fructosamine or 1-amino-DOOA-gluconamide) were prepared by diluting 1 mg/mL stock solutions in 0.1 M sodium bicarbonate buffer pH 8.5 at known concentrations of amine (10 to 50 µg/mL). Various volumes of a fresh solution of 0.01 % TNBS (w/v) in the same buffer were added in each solution, in order to get a molar ratio of TNBS/amine of 1, and samples were incubated at 37 °C for 2 h. Then, the product of reaction between the amine and TNBS was analyzed by UV spectroscopy (from 580 to 280 nm) after addition of a small volume of 1 M HCl (150 µL) in the samples. The same procedure was used to quantify amines during the amide coupling reactions with HA, by taking small aliquots of the reaction medium as a function of time.

Procedure for determining the DS from the kinetics of amide coupling reactions

From the UV spectra recorded for fructosamine-TNB (1-amino-DOOA-gluconamide-TNB) derivatives, a standard curve was plotted with the maximal absorbance values (curves (a) in Figure S7). It is important to note that the wavelength of the maximal absorbance depends on the primary amines. This allowed us to determine the amount of unreacted primary amines during the amide coupling reaction with HA using an amine/HA molar ratio of 0.15 to 0.2. From the kinetic curves, we estimated approximately 100 % of conversion for HA-fructose and 65 % for HA-gluconamide within 24 h and 65 h, which gave values of DS of 0.15 and 0.1, respectively (curve (b) in Figure S7).

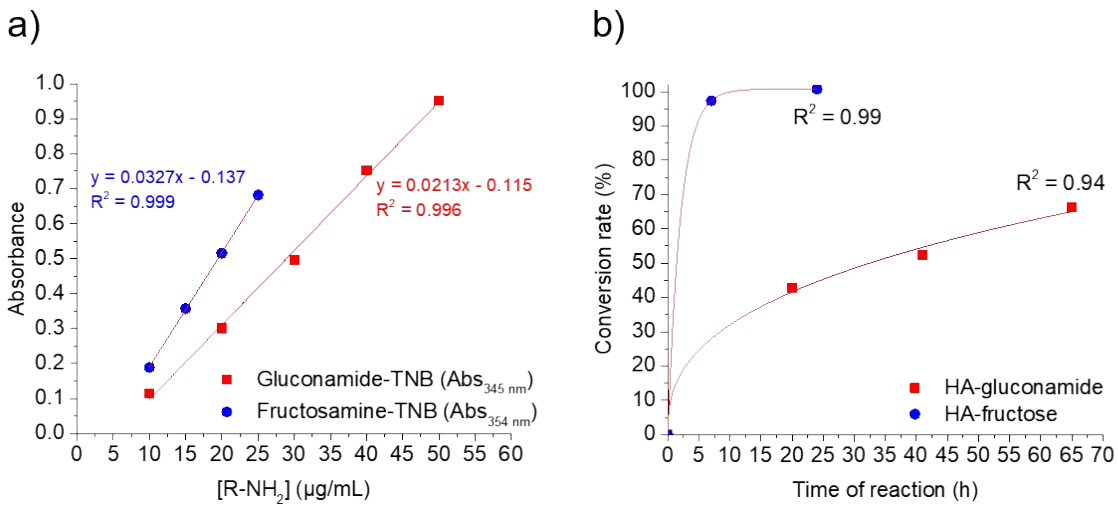

Figure S7. Reaction kinetics for the syntheses of HA-gluconamide and HA-fructose. Standard curves with the respective equations used to quantify the free amines (a), and kinetic curves plotted for the coupling reactions of fructosamine and gluconamide with HA (curve fitting by non-linear fit models using Origin 2015 software).

7. Preparation of HA-PBA (HA-BOR) and HA-saccharide mixtures

The different HA derivatives were solubilized in 0.01 M HEPES buffer containing 0.15 M NaCl pH 7.4. The dissolution time was at least 12 h at 4 °C. The solutions of HA-BOR or HA-PBA and of HA-saccharide (HA-fructose, HA-maltose, HA-glucose or HA-gluconamide) were mixed under vigorous stirring at room temperature, at a total polymer concentration of 15 g/L and with BOR or PBA/sugar molar ratio of 1. The mixtures were then allowed to rest at 4 °C overnight before rheological analysis.

8. Dynamic rheological behavior of the HA-PBA (BOR) conjugates alone

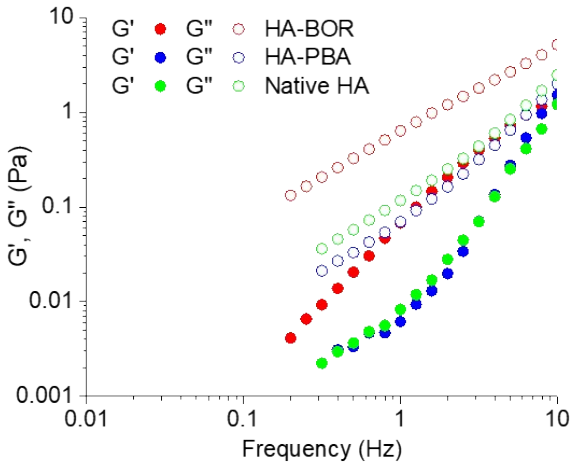

Figure S8. Frequency dependence of storage (G') and loss (G") moduli of the HA-PBA and HA-BOR derivatives alone at pH 7.4, compared to native HA; closed symbols: G' curves; open symbols: G'' curves.

9. Methodology for K_a measurements by ^{1}H NMR spectroscopy

The procedure to determine the K_a values was adapted from previous studies using free boronic acids and saccharides.[21,22] This method consisted in assuming that a boronic acid (B) and a saccharide (S) bind in one modality, BS:

$$B + S \rightleftarrows BS$$

$$K_a = \frac{[BS]}{[B].[S]} \quad (1)$$

Where [B], [S] and [BS] are the molar concentrations of the free boronic acid, the free saccharide and the complex, respectively.

To determine K_a, the [BS]/[B] ratio was determined by digital integration of the aryl protons of the boronic acid/saccharide complex and of the free boronic acid. This allowed determination of [B], [BS] and [S], as follows:

$$[B] = \frac{[B]_0}{\frac{[BS]}{[B]} + 1} \quad (2)$$

Where $[B]_0$ is the initial concentration of boronic acid added in the NMR tube, and

$$[BS] = \frac{[BS]}{[B]}[B] \quad (3)$$

$$[S] = [S]_0 - [BS] \quad (4)$$

Where $[S]_0$ is the initial concentration of saccharide added in the NMR tube.

Procedure for the preparation of samples for NMR analysis

Stock solutions of APBA (ABOR) and free (grafted) saccharides were prepared by solubilization in distilled water. When necessary, the pH was carefully adjusted to 7.4 by adding 1 M NaOH, using a pH-meter, and water was added to get concentrations ranging from 4 to 60 mM. Then, the solutions were diluted with 0.02 M PBS pH 7.4 in order to obtain final concentrations of 2 to 30mM APBA (ABOR) or saccharide in 0.01 M PBS at pH 7.4.The solutions of complexes were then prepared by mixing various volumes of a stock solution of APBA (ABOR) with a stock solution of a respective free (grafted) saccharide. This generated mixtures at pH 7.4 (± 0.1), with a APBA (ABOR)/saccharide molar ratio ranging from 0.3 to 1.5. Water was removed by freeze-drying and the samples were properly dissolved in D_2O prior to NMR analysis. Each value of K_a was determined from two experiments of titration using freshly prepared solutions. ^{1}H NMR titration was performed with at least 6 different concentrations at 25 °C.

Procedure for determining the chemical shifts of aryl protons of bound and free boronic acids

^{1}H NMR spectra of APBA and ABOR alone were first recorded (spectra (a) in Figure S9-S12, S17-S20 and S24-S27). Second, ^{1}H NMR spectra of APBA and ABOR in the presence of excess free saccharide (fructose or gluconamide derivative which is free in solution) to induce 100 % complex formation are acquired (spectra (b) in Figure S9-S10 and S24-S25). Comparison of spectra (a) and (b) allows the assignment of the aryl protons of bound and free boronic acids. This analysis was then used to interpret the spectra from the titrations with sugars (fructose, maltose or gluconamide derivative which are free in solution or grafted on HA; spectra (c) in Figure S9-S10 and S24-S25 or spectra (b) in Figure S11-S12, S17-S20 and S26-S27).

10. Determination of K_a by ^{1}H NMR for APBA (ABOR) and fructose (free fructose and HA-fructose)

As the bound and unbound forms of APBA (ABOR) in the presence of fructose are distinguishable by 1H NMR spectroscopy,[21,23] this technique was used to evaluate directly the affinity of APBA and ABOR for free D-fructose and grafted fructose (Figure S9-S12) as well as to measure the rate of exchange between the free and bound states (Figure S13 and S14).

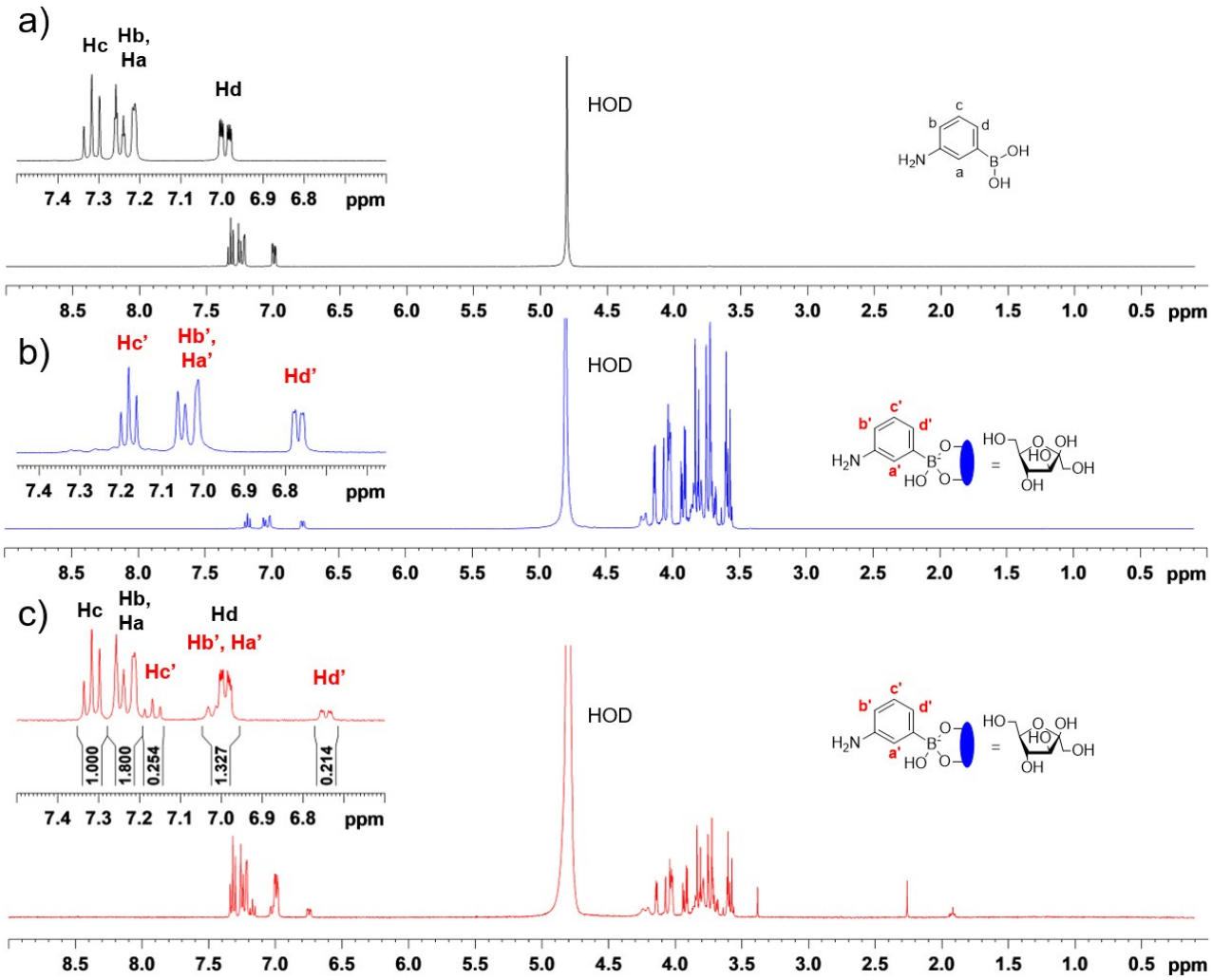

Figure S9. ^{1}H NMR spectra in 0.01 M deuterated PBS pH 7.4 at 25 °C of APBA alone (15 mM) (a), APBA (15 mM) in the presence of excess D-fructose (150 mM) (b), and APBA (15 mM) with D-fructose (15 mM) (c). The [BS]/[B] ratio was determined from the digital integration of Hc (free APBA) and Hd' (complexed APBA) signals.

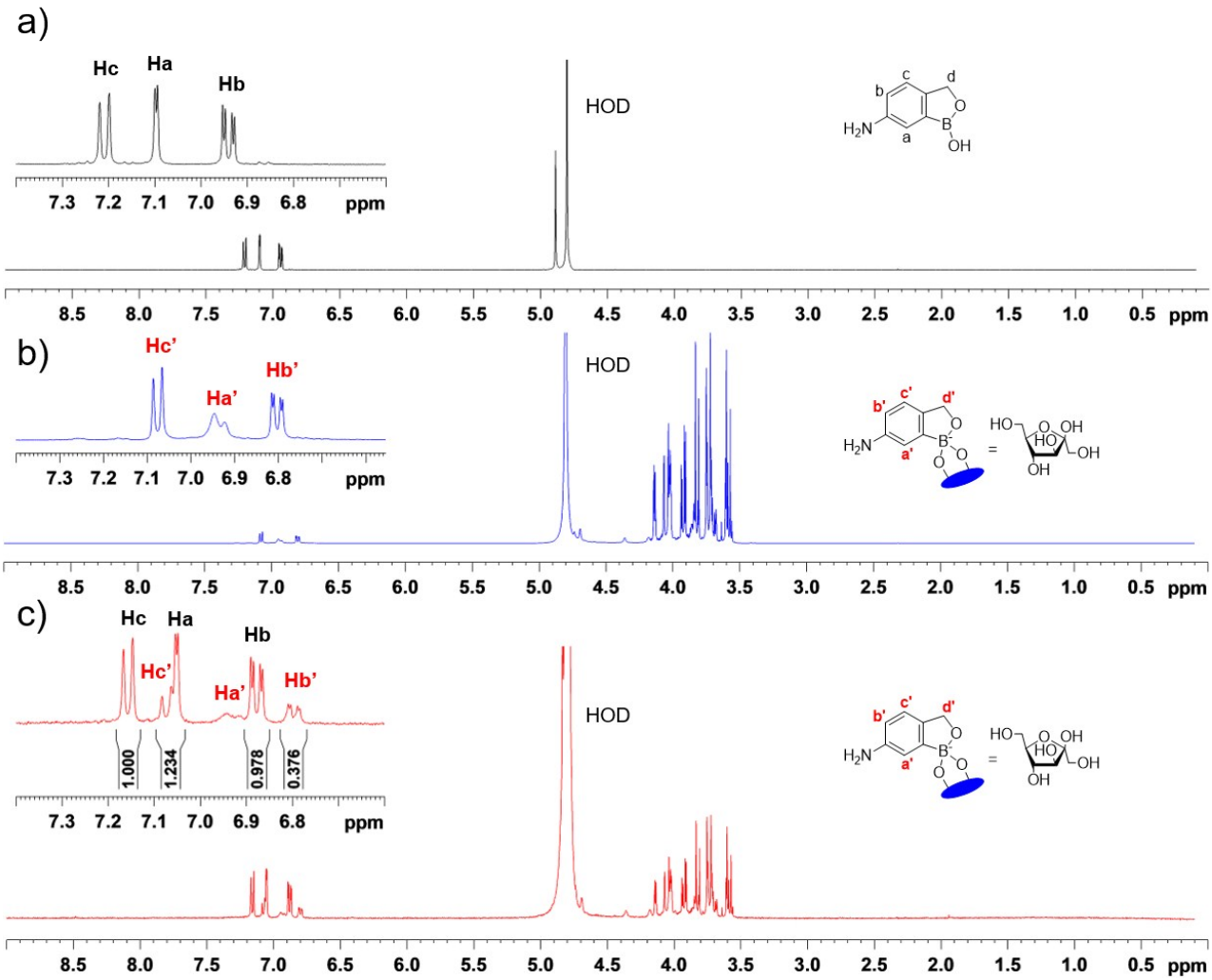

Figure S10. ^{1}H NMR spectra in 0.01 M deuterated PBS pH 7.4 at 25 °C of ABOR alone (15 mM) (a), ABOR (15mM) in the presence of excess D-fructose (150 mM) (b), and ABOR (15 mM) with D-fructose (15 mM) (c). The [BS]/[B] ratio was determined from the digital integration of Hc (free ABOR) and Hb' (complexed ABOR) signals.

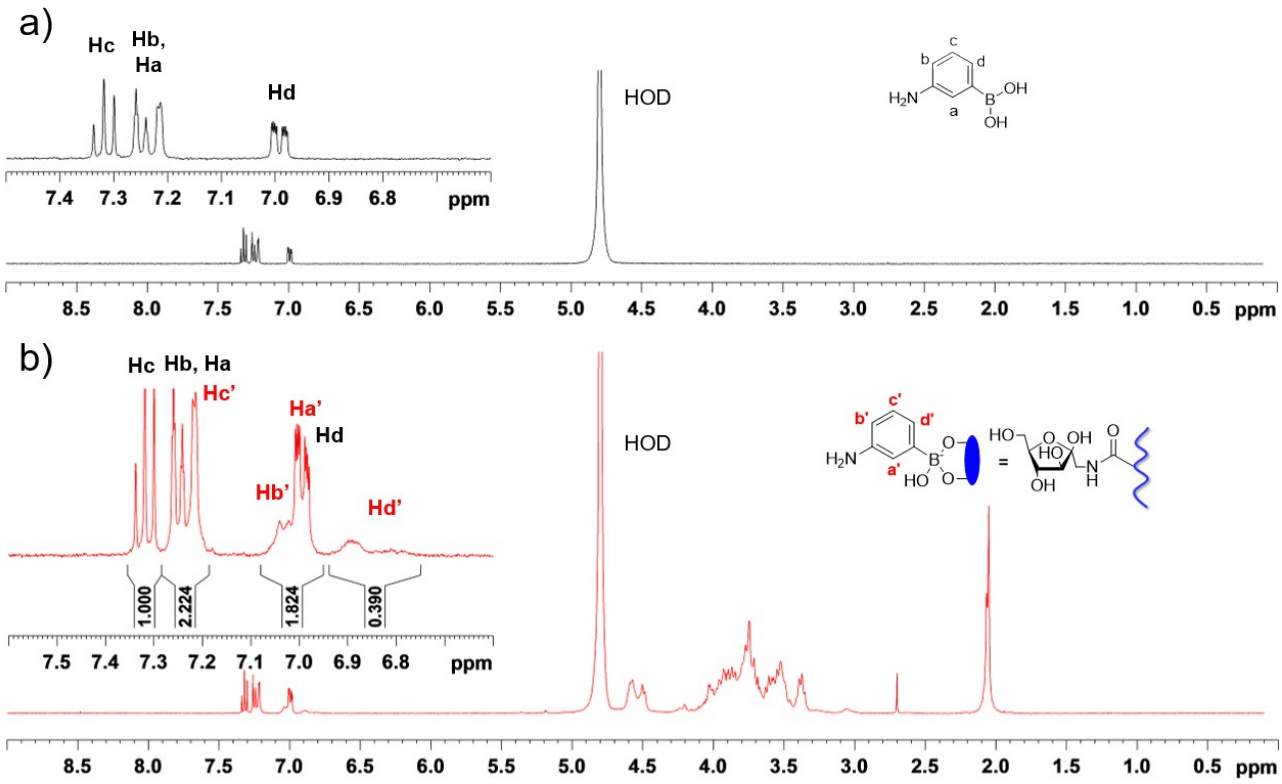

Figure S11. ^{1}H NMR spectra in 0.01 M deuterated PBS pH 7.4 at 25 °C of APBA alone (1 mM) (a) and APBA (1 mM) with D-fructose (1 mM of grafted fructose) (b). Similar to free D-fructose, the [BS]/[B] ratio was determined from the digital integration of Hc (free APBA) and Hd' (complexed APBA) signals.

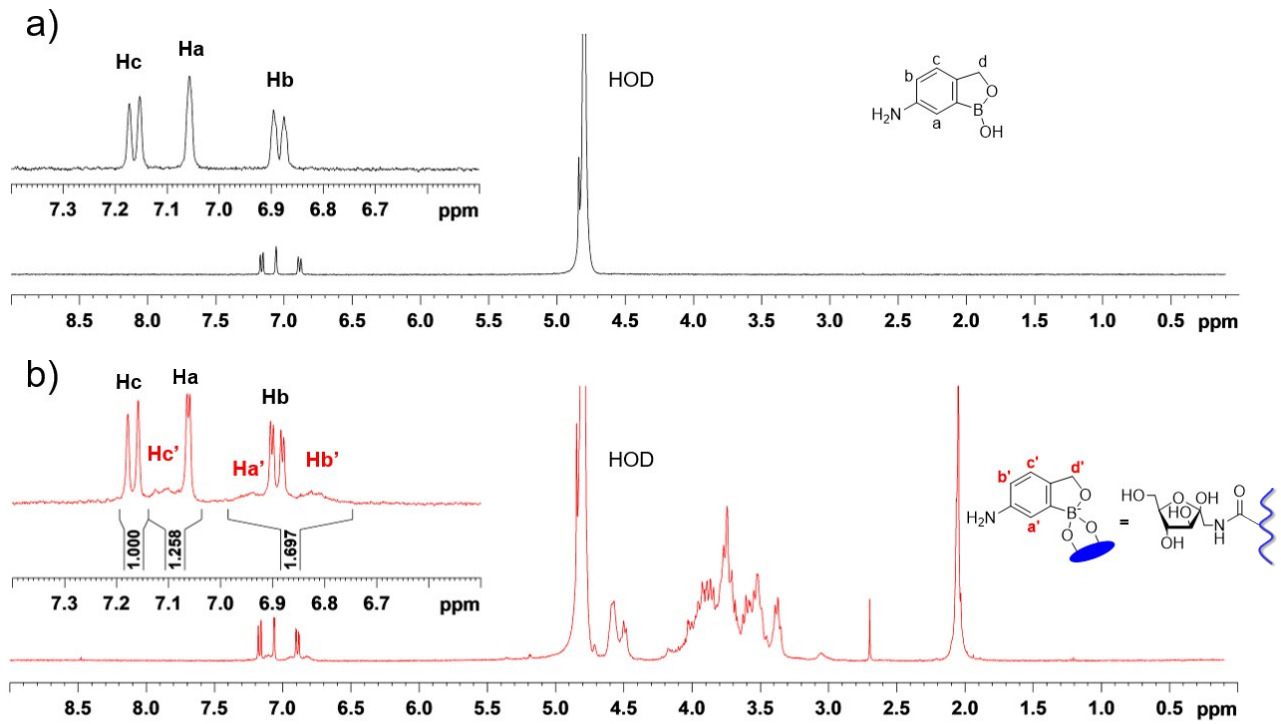

Figure S12. ^{1}H NMR spectra in 0.01 M deuterated PBS pH 7.4 at 25 °C of ABOR alone (1mM) (a) and ABOR (1mM) with HA-fructose (1 mM of grafted fructose) (b). Similar to free D-fructose, the [BS]/[B] ratio was determined from the digital integration of Hc (free ABOR) and Hb, Ha', Hb' (3H, free and complexed ABOR) signals.

11. Methodology for k_{ex} measurement by 2D EXSY (EXchange SpectroscopY)

The k_{ex} values for slow exchange systems were determined from EXSY experiments, set up with at least 3 different mixing times (d8) among 0.8, 1, 1.2 and 1.5 s.[24] Solutions of APBA (ABOR) and saccharides were prepared as previously described for K_a measurements by ^{1}H NMR titration. From the 2D spectra of APBA (ABOR) in the presence of 0.6 molar equivalent of saccharide, the diagonal and cross-peaks for the bound and unbound aromatic resonances of APBA (ABOR) were carefully integrated, and the integration values were used to determine k_{ex} by using the following equation[25]

$$ln\frac{(r+1)}{(r-1)} = k_{ex}\tau_m \quad (5)$$

where τ_m is the mixing time and r is defined by the following equation

$$r = \frac{4\chi_c\chi_f\,(I_{HH} + I_{H'H'})}{(I_{HH'} + I_{H'H})} - (\chi_c - \chi_f)^2 \quad (6)$$

where χ_c and χ_f are the mole fraction of complexed and free APBA (ABOR), respectively, with χ_c = 0.4 and χ_f = 0.6. $I_{HH'}$ and $I_{H'H}$ are the intensities of the cross peaks between a ^{1}H signal of free and complexed APBA (ABOR), respectively, whereas I_{HH} and $I_{H'H'}$ are the intensities of the diagonal peaks.

12. Determination of k_{ex} by 2D EXSY for APBA (ABOR) and free fructose

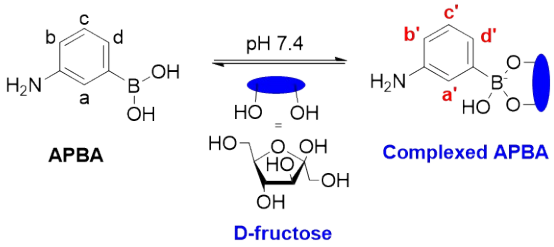

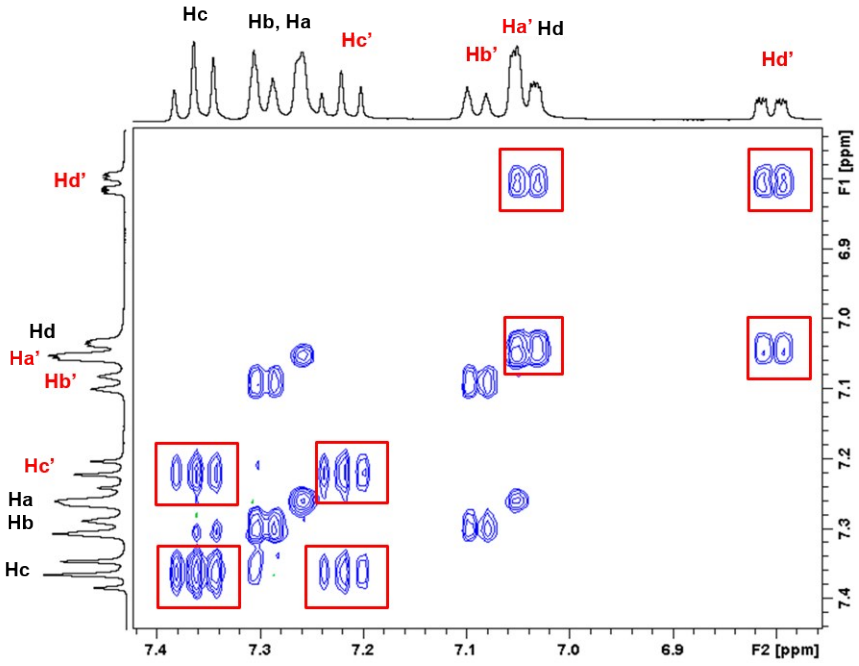

Figure S13. 2D EXSY spectra at 25 °C of APBA (18 mM) with D-fructose (12 mM) in 0.01 M deuterated PBS pH 7.4 (τ_m = 1.5 s). k_{ex} was determined from the digital integration of the diagonal peaks (Hcc, Hc'c' and Hdd, Hd'd') and of the cross peaks (Hcc', Hc'c and Hdd', Hd'd) of APBA.

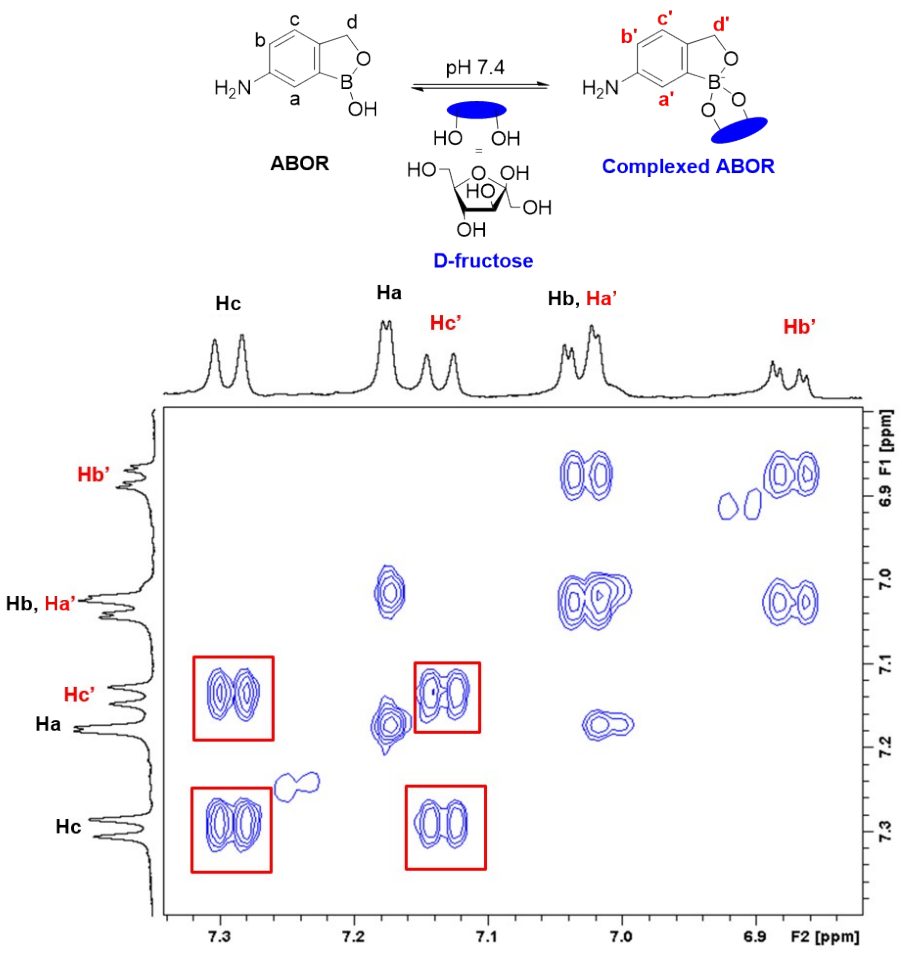

Figure S14. 2D EXSY spectra at 25 °C of ABOR (18 mM) with D-fructose (12 mM) in 0.01 M deuterated PBS pH 7.4 (τ_m = 1.5 s). k_{ex} was determined from the digital integration of the diagonal peaks (Hcc, Hc'c') and of the cross peaks (Hcc', Hc'c) of ABOR.

13. Calorimetric titration of APBA (ABOR) with maltose-COOH

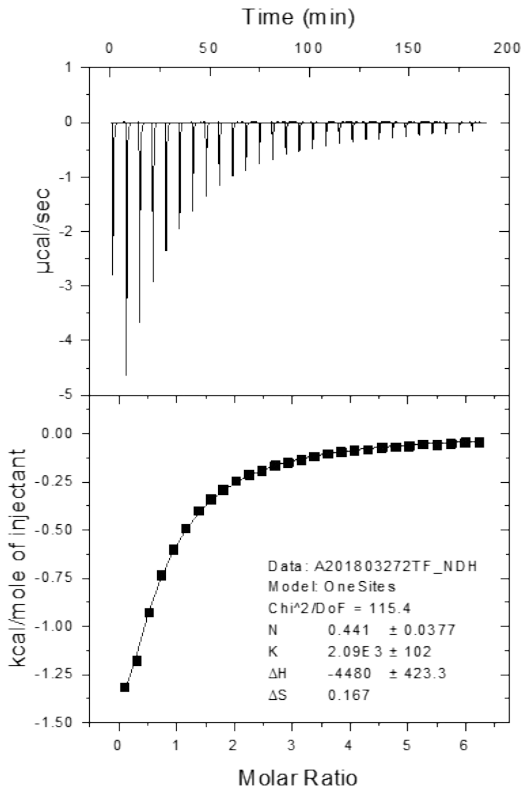

Figure S15. Calorimetric titration of maltose-COOH (0.5 mM) with APBA (15 mM) in 0.01 M PBS (pH 7.4, 25 °C).

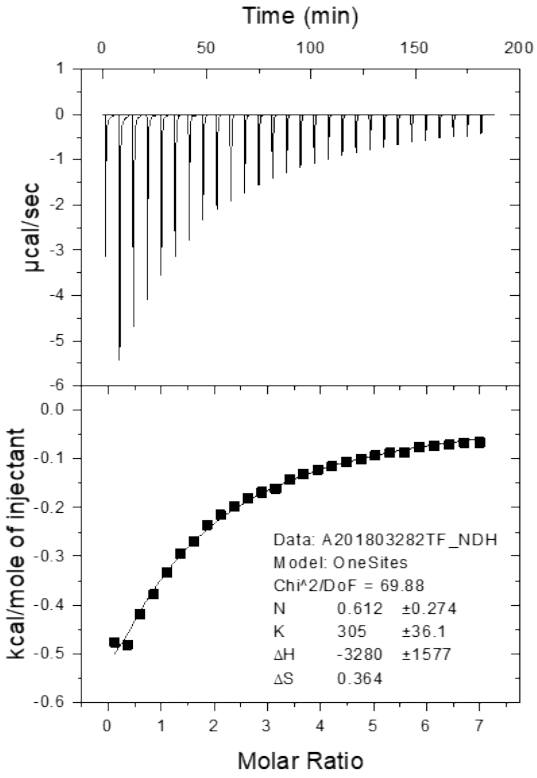

Figure S16. Calorimetric titration of maltose-COOH (1 mM) with ABOR (35 mM) in 0.01 M PBS (pH 7.4, 25 °C).

14. Determination of K_a by ^{1}H NMR for APBA (ABOR) and maltose derivatives (maltose-COOH and maltose grafted on HA)

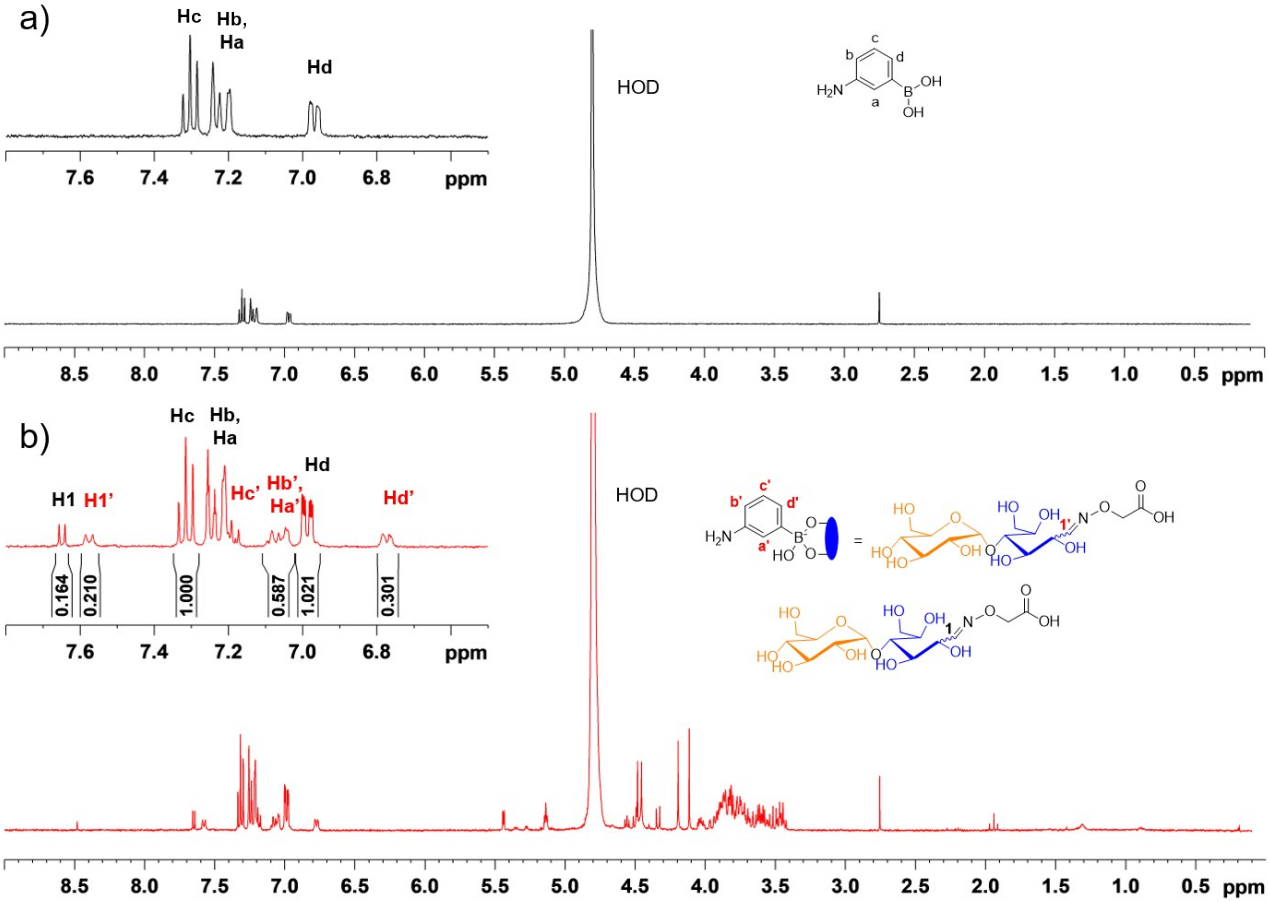

Figure S17. ^{1}H NMR spectra in 0.01 M deuterated PBS pH 7.4 at 25 °C of APBA alone (1 mM) (a) and APBA (1 mM) with maltose-COOH (1 mM) (b). Assuming a 2:1 stoichiometry for the APBA/maltose-COOH complex, K_a could not be determined because the concentration of molecules used was too low to apply equations related to 1:2 equilibria[26] (H1 and H1' correspond to free and bound maltose-COOH, respectively).

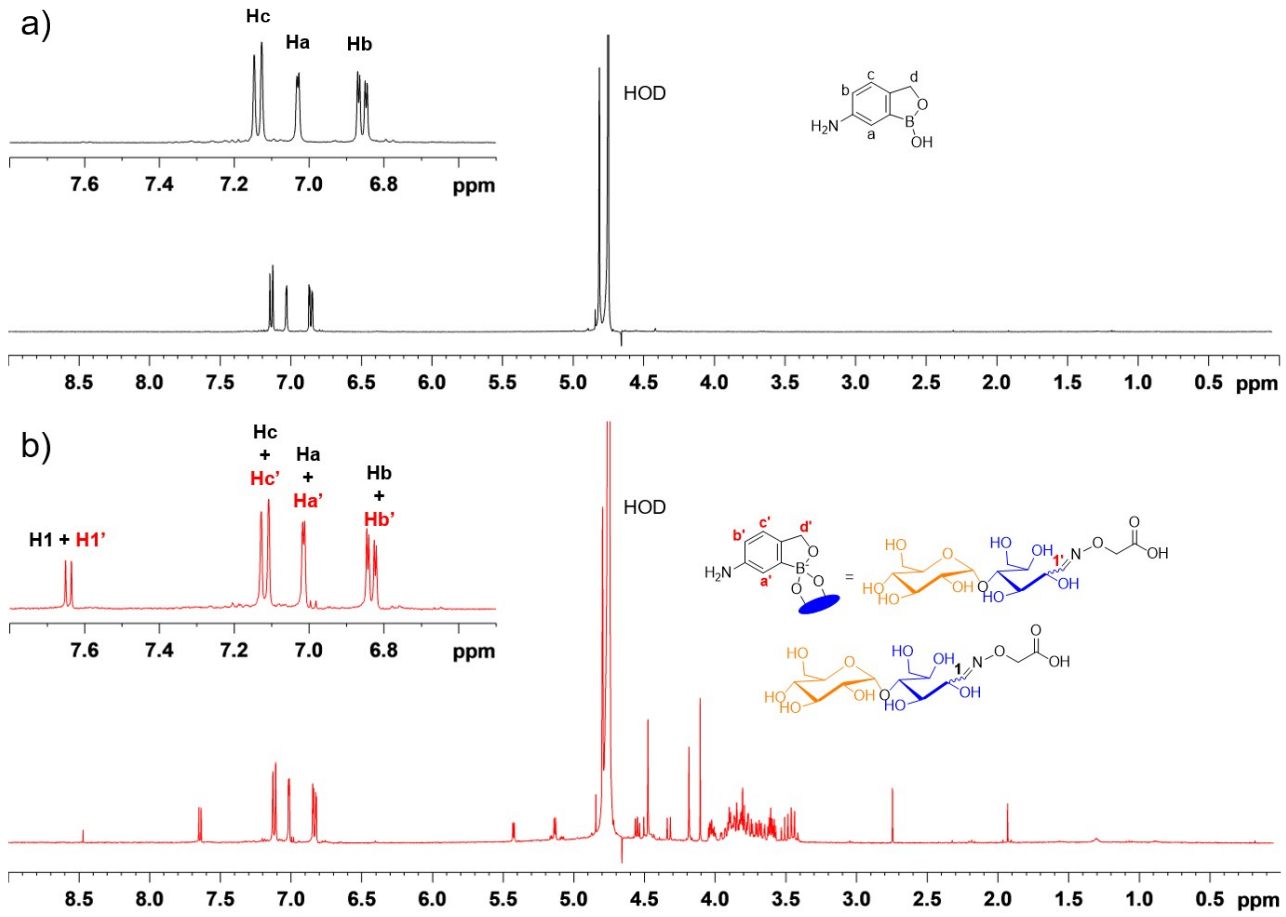

Figure S18. ^{1}H NMR spectra in 0.01 M deuterated PBS pH 7.4 at 25 °C of ABOR alone (1 mM) (a) and ABOR (1 mM) with maltose-COOH (1 mM) (b). K_a was not measured because of rapid exchange dynamics relative to NMR time-scale (mainly ^{1}H signals from free ABOR are observed at 25 °C; H1 and H1' correspond to free and bound maltose-COOH, respectively).

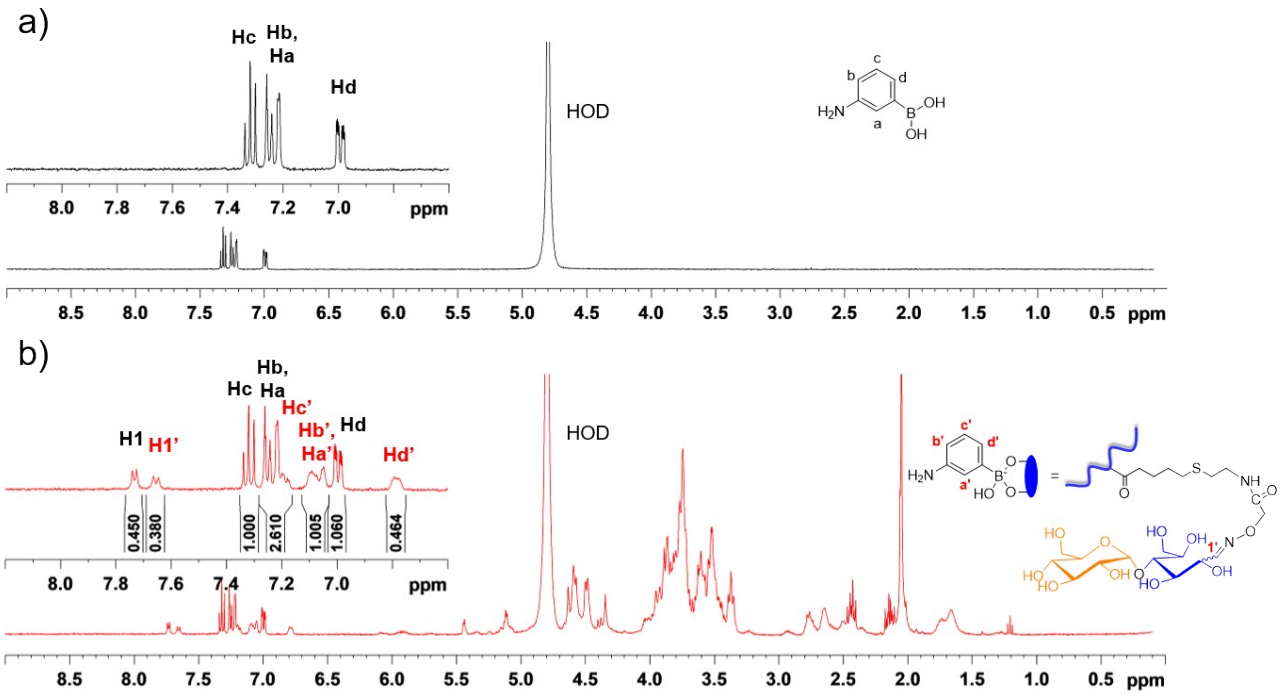

Figure S19. [1]H NMR spectra in 0.01 M deuterated PBS pH 7.4 at 25 °C of APBA alone (1 mM) (a) and APBA (1 mM) with HA-maltose (1 mM of grafted maltose) (b). Assuming a 1:1 stoichiometry of APBA/HA-maltose, the [BS]/[B] ratio was determined from the digital integration of Hc (free APBA) and Hd' (complexed APBA) signals (similar to the NMR spectrum of APBA/maltose-COOH, H1 and H1' correspond to free and bound HA-maltose, respectively).

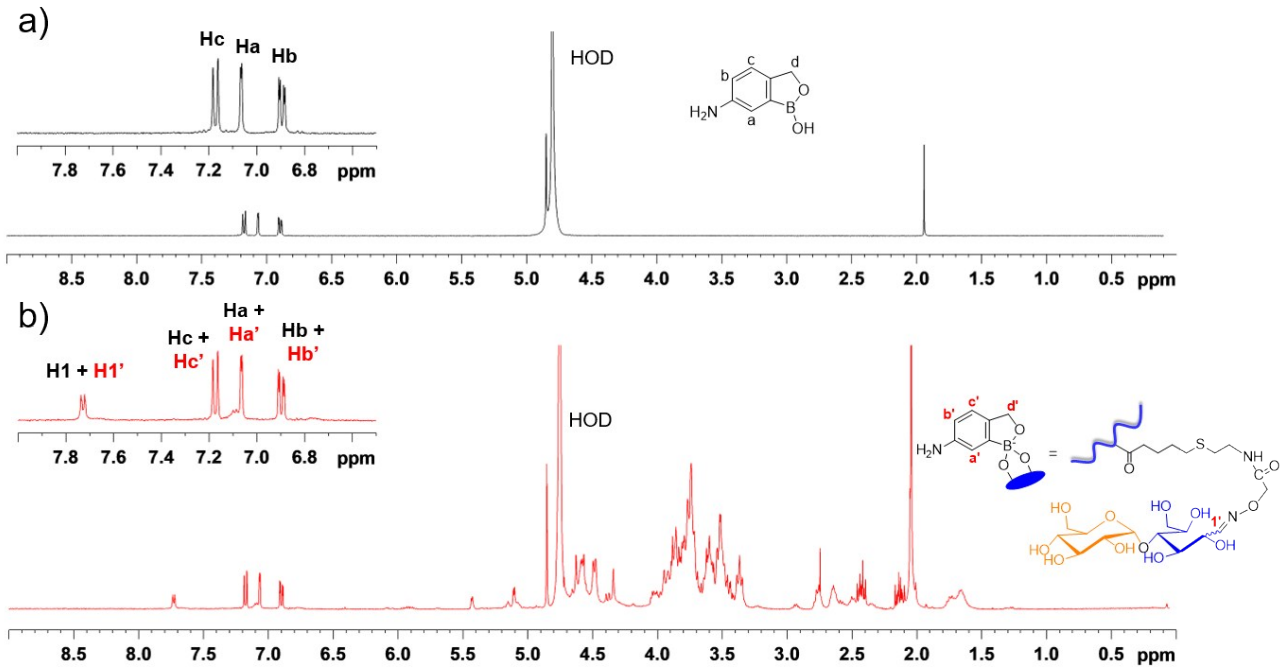

Figure S20. [1]H NMR spectra in 0.01 M deuterated PBS pH 7.4 at 25 °C of ABOR alone (1 mM) (a) and ABOR (1 mM) with HA-maltose (1 mM of grafted maltose) (b). Similar to maltose-COOH, K_a was not measured because of rapid exchange dynamics relative to NMR time-scale (mainly [1]H signals from free ABOR are observed at 25 °C; similar to the NMR spectrum of ABOR/maltose-COOH, H1 and H1' correspond to free and bound HA-maltose, respectively).

15. Determination of k_{ex} by 2D EXSY for APBA and HA-maltose

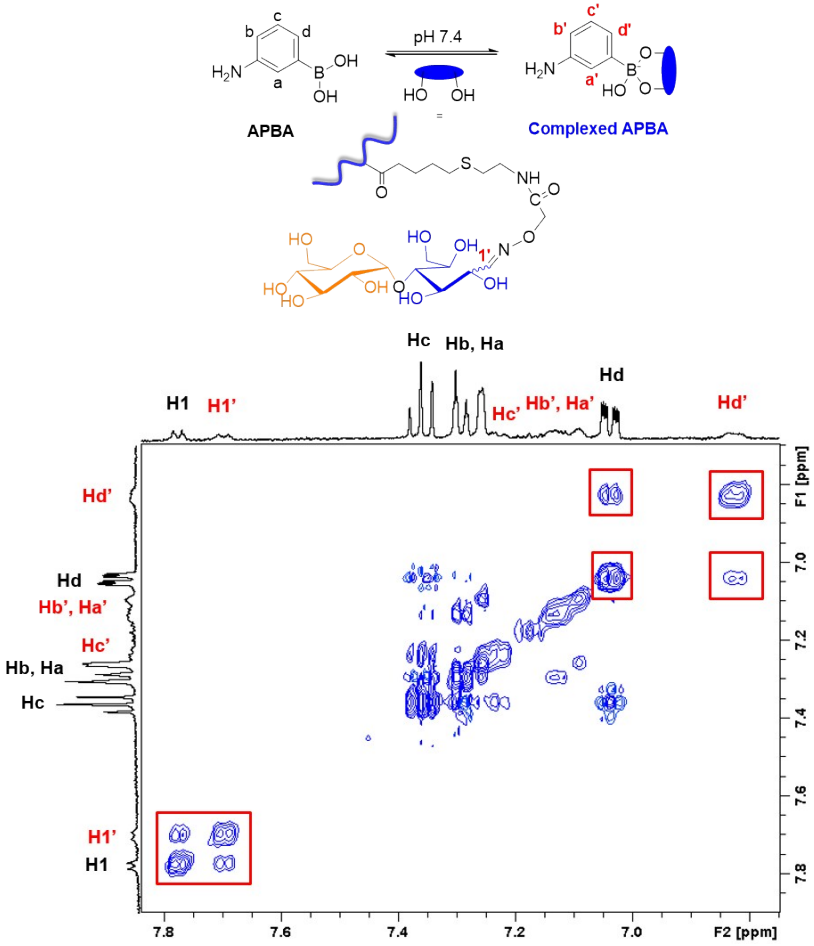

Figure S21. 2D EXSY spectra at 25 °C of APBA (1.2mM) with HA-maltose (0.8mM grafted maltose) in 0.01 M deuterated PBS pH 7.4 (τ_m = 1.5 s). k_{ex} was determined from the digital integration of the diagonal peaks (Hdd, Hd'd') and of the cross peaks (Hdd', Hd'd) of APBA, and of the diagonal peaks (H11, H1'1') and cross peaks (H11', H1'1) of grafted maltose.

16. Methodology for k_{ex} measurement by variable-temperature NMR spectroscopy

The molecular exchange rate constants at the coalescence temperature were estimated for ABOR in the presence of one molar equivalent of free or grafted maltose, using the following approximate expression[25,26]

$$k_c = \frac{\pi \Delta \nu}{\sqrt{2}} \quad (7)$$

where k_c is the molecular exchange rate constant at a coalescence temperature and $\Delta \nu$ is the chemical shift difference between the signal of free (Hb) and complexed (Hb') ABOR (and/or of free (H1) and complexed (H1') maltose) determined from the ^{1}H NMR spectra of the mixtures far below coalescence (1 °C). The extrapolated exchange rate constant k_{ex} at 25 °C was then obtained from the Eyring equation

$$k\mathrm{ex} = \left(\frac{k\mathrm{b}T}{h}\right)\exp\left(-\frac{\Delta G \neq}{RT}\right) \quad (8)$$

where k_b is the Boltzmann constant, T is the absolute temperature, h is the Plank constant, $\Delta G^{\neq}$ is the free energy of activation for the molecular exchange and R is the gas constant.

17. Determination of k_{ex} by variable-temperature NMR spectroscopy for ABOR/maltose-COOH or HA-maltose

In NMR experiments, the exchange signals for ABOR/free maltose and ABOR/grafted maltose coalesced at 15 °C (Figure S22 and S23), which allowed estimating the molecular exchange rate constant at the coalescence temperature.[27,28] From these experiments, the extrapolated exchange rate constant k_{ex} at 25 °C of ABOR/free maltose and ABOR/grafted maltose were found to be 184 and 191 s^{-1}, respectively.

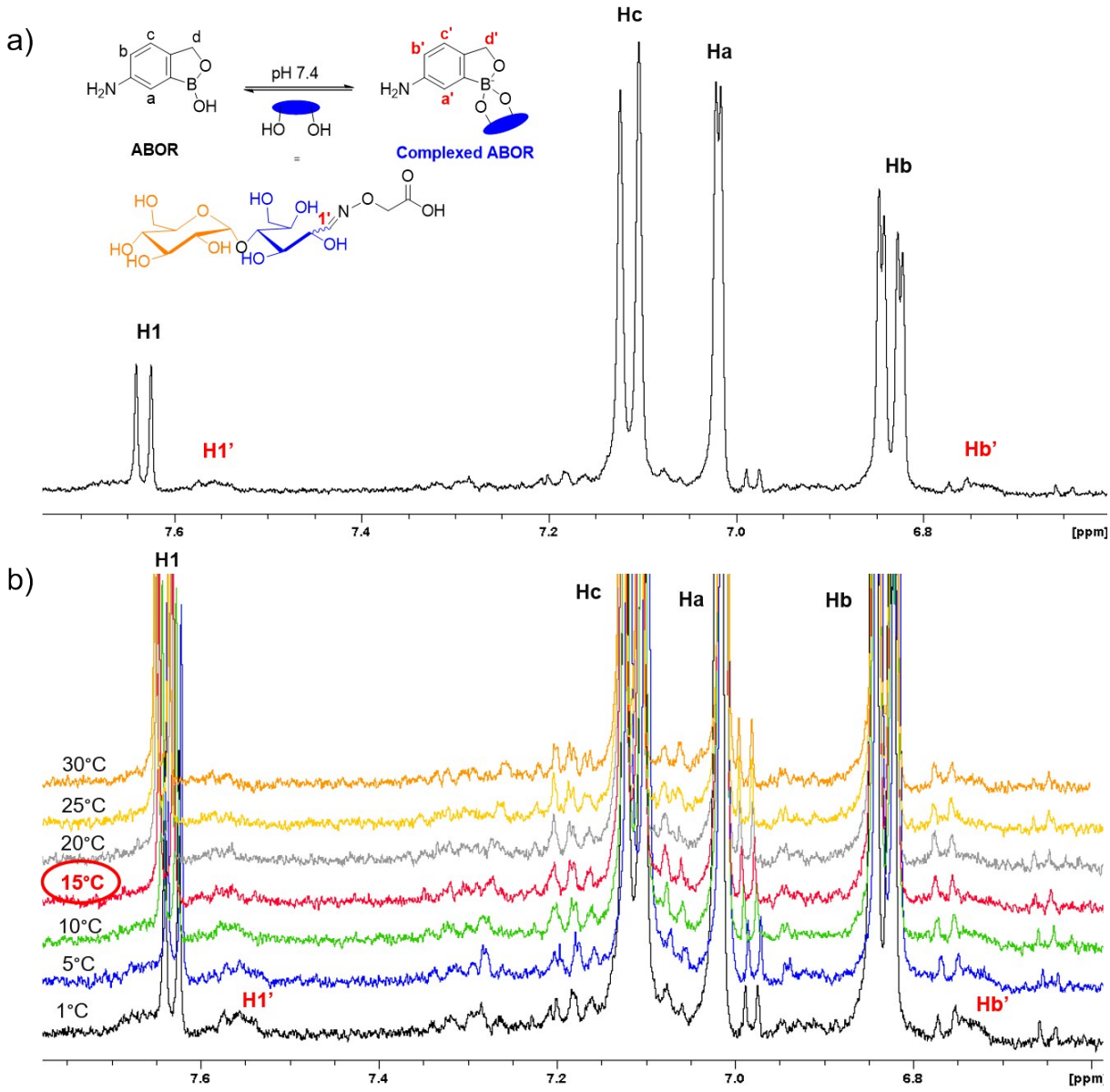

Figure S22. Variable-temperature ^{1}H NMR analysis of ABOR/maltose-COOH (at a molar ratio of 1/1), in 0.01 M deuterated PBS pH 7.4: ^{1}H NMR spectrum of the complex far below coalescence (1 °C) (a), and ^{1}H NMR spectra at different temperatures (b). k_{ex} was determined following equations 7 and 8, using the chemical shifts of Hb and Hb' (free and complexed ABOR) and/or H1 and H1' (free and complexed maltose) at 1 °C. Of note, the existence of other complexes cannot be excluded as small additional signals are also observed in the NMR spectra.

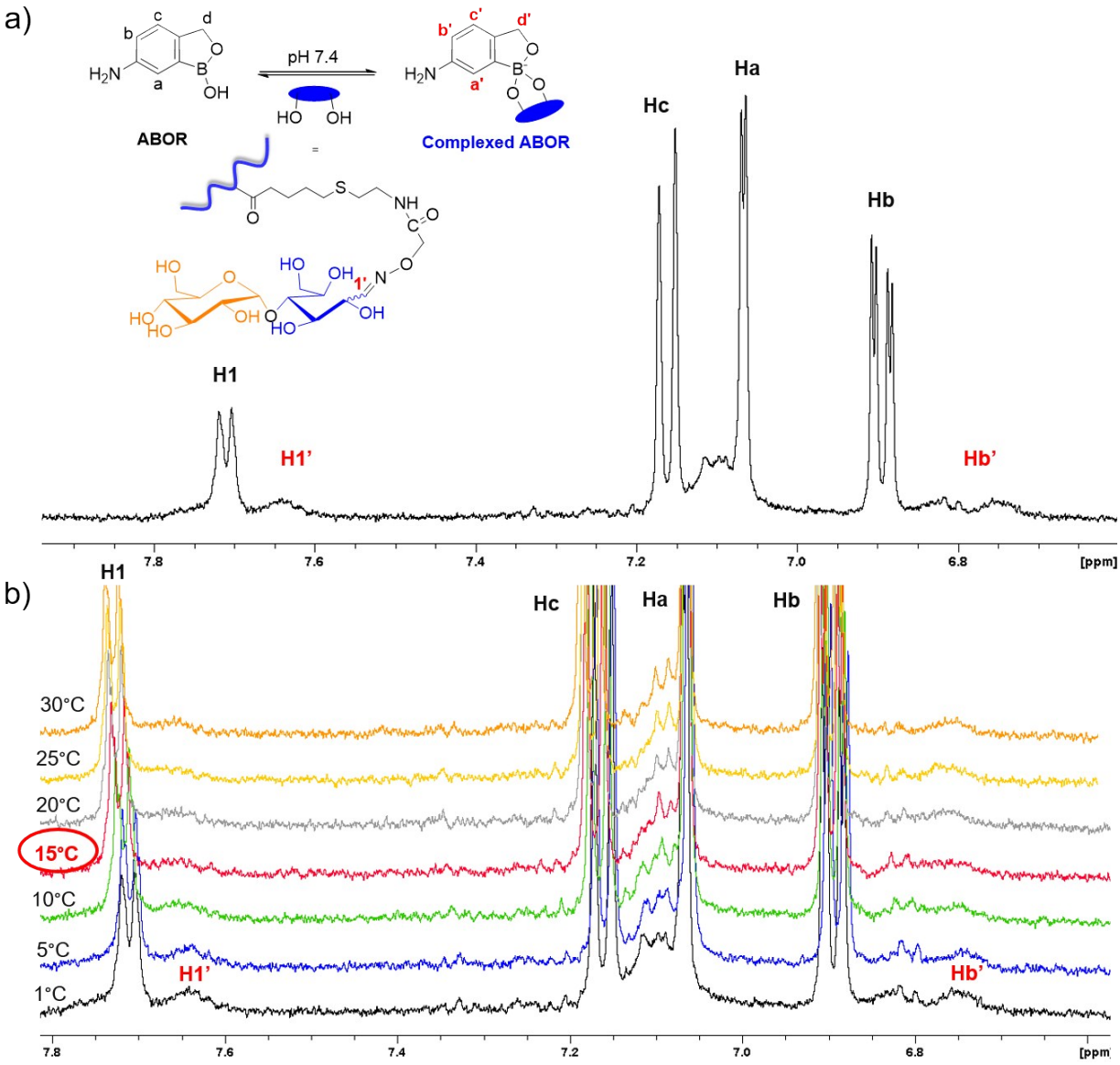

Figure S23. Variable-temperature ^{1}H NMR analysis of ABOR/HA-maltose (at a molar ratio of 1 ABOR/1 maltose), in 0.01 M deuterated PBS pH 7.4: ^{1}H NMR spectrum of the complex far below coalescence (1 °C) (a), and ^{1}H NMR spectra at different temperatures (b). Similar to maltose-COOH, k_{ex} was determined following equations 7 and 8, using the chemical shifts of Hb and Hb' (free and complexed ABOR) and/or H1 and H1' (free and complexed maltose) at 1 °C. Of note, the existence of other complexes cannot be excluded as small additional signals are also observed in the NMR spectra.

18. Determination of K_a by ^{1}H NMR for APBA (ABOR) and gluconamide derivatives (free gluconamide and HA-gluconamide)

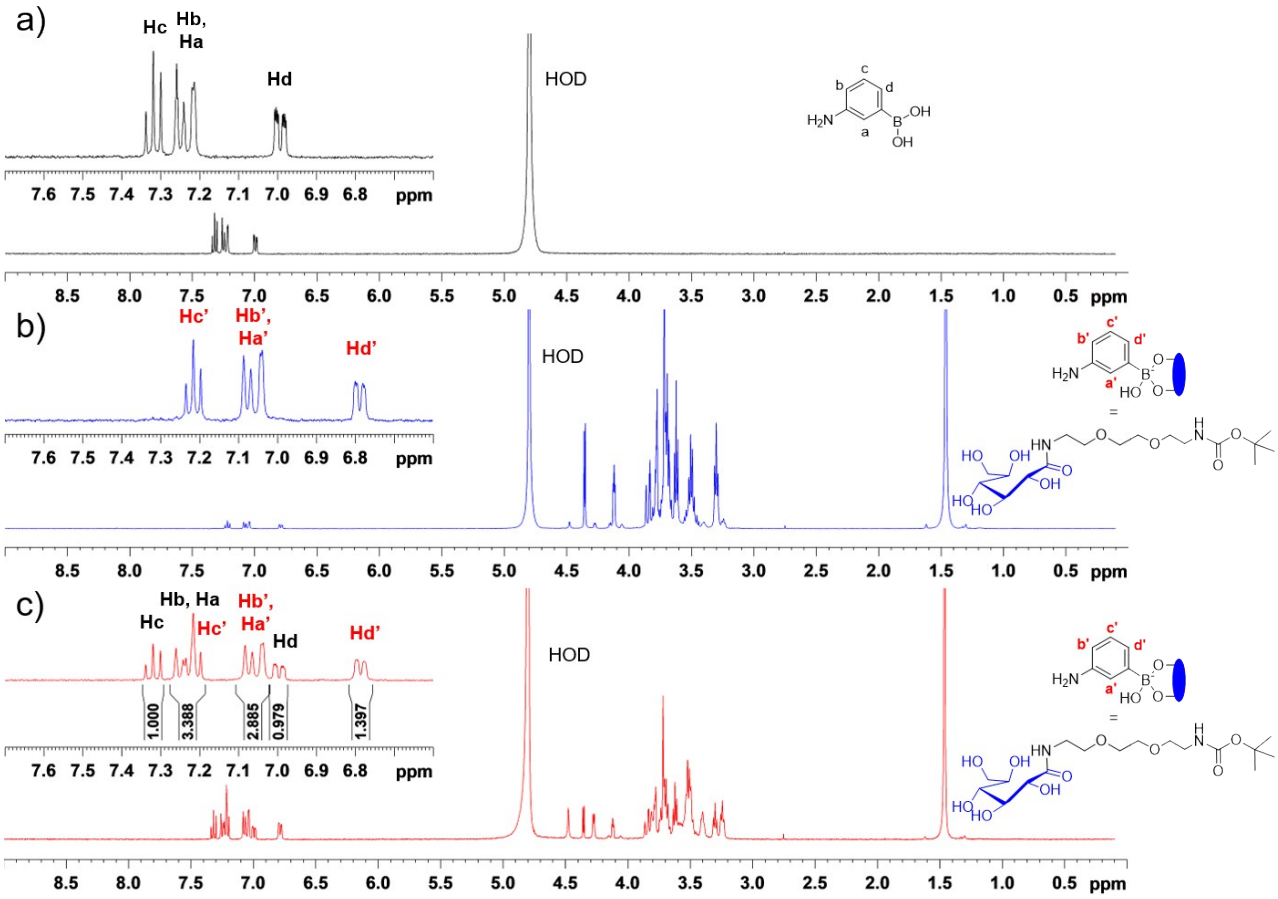

Figure S24. ^{1}H NMR spectra in 0.01 M deuterated PBS pH 7.4 at 25 °C of APBA alone (1 mM) (a), APBA (1 mM) in the presence of excess free gluconamide (10 mM) (b), and APBA (1 mM) with free gluconamide (1 mM) (c). The [BS]/[B] ratio was determined from the digital integration of Hc (free APBA) and Hd' (complexed APBA) signals.

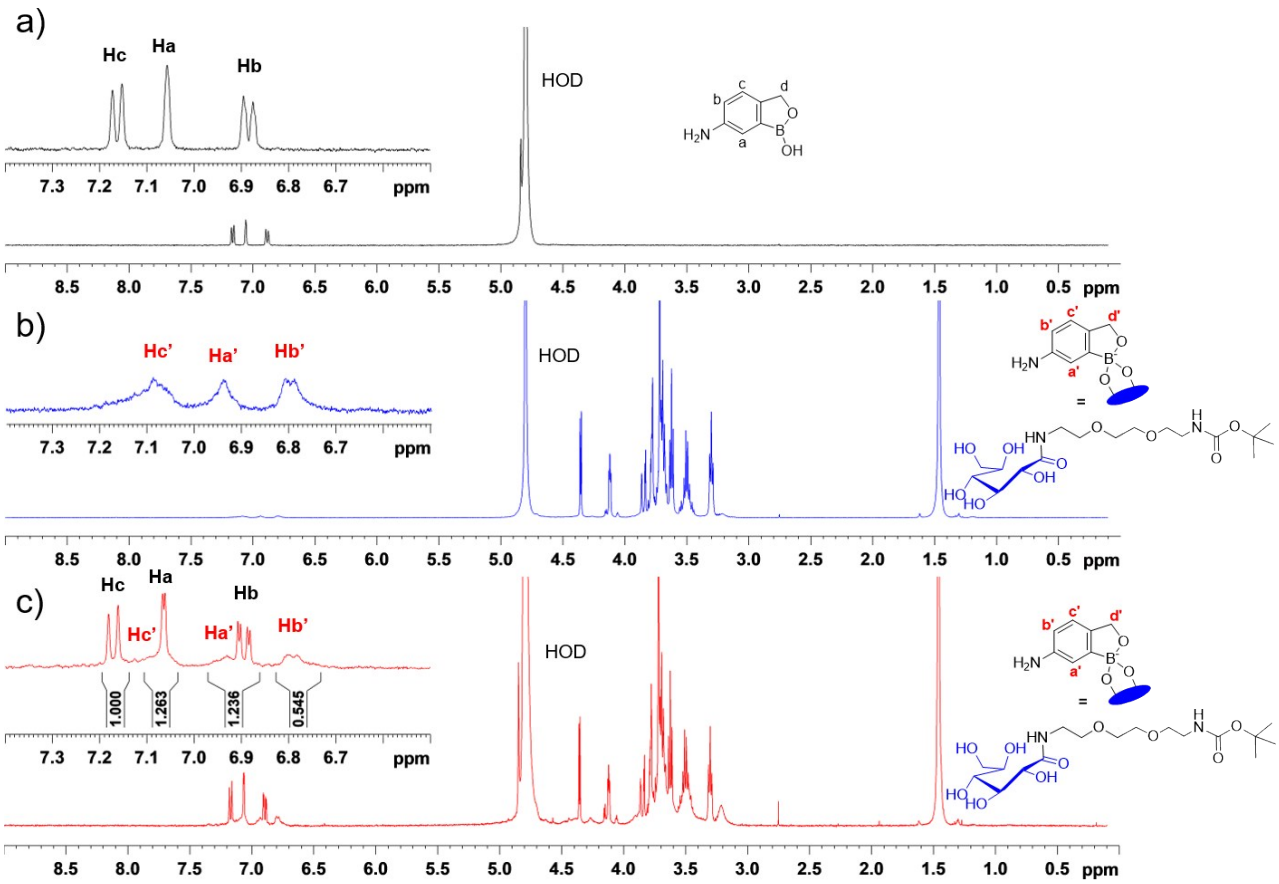

Figure S25. ^{1}H NMR spectra in 0.01 M deuterated PBS pH 7.4 at 25 °C of ABOR alone (1 mM) (a), ABOR (1 mM) in the presence of excess free gluconamide (10 mM) (b), and ABOR (1 mM) with free gluconamide (1 mM) (c). Compared to the maltose derivatives, the bound and unbound forms of gluconamide are in a slower exchange relative to the NMR time-scale, which allowed determination of the [BS]/[B] ratio from the digital integration of Hc (free ABOR) and Hb' (complexed ABOR) signals.

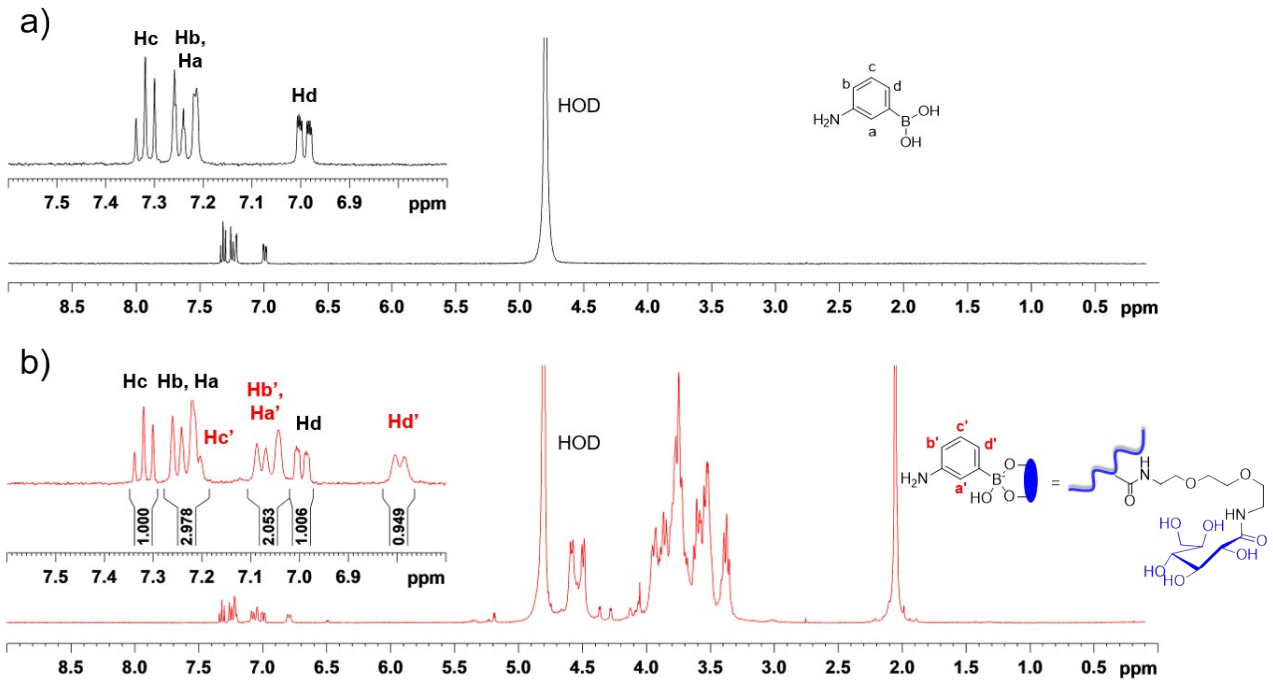

Figure S26. [1]H NMR spectra in 0.01 M deuterated PBS pH 7.4 at 25 °C of APBA alone (1 mM) (a) and APBA (1 mM) with HA-gluconamide (1 mM of grafted gluconamide) (b). Similar to the free gluconamide derivative, the [BS]/[B] ratio was determined from the digital integration of Hc (free APBA) and Hd' (complexed APBA) signals.

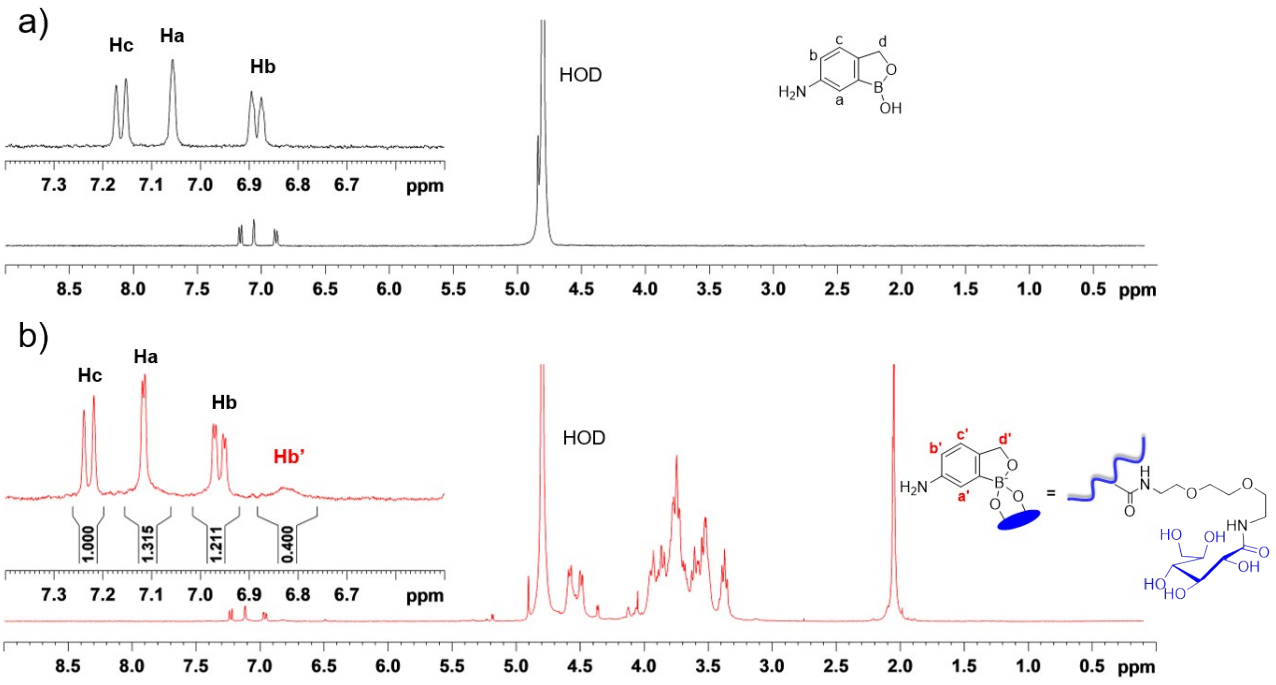

Figure S27. [1]H NMR spectra in 0.01 M deuterated PBS pH 7.4 at 25 °C of ABOR alone (1 mM) (a) and ABOR (1 mM) with HA-gluconamide (1 mM of grafted gluconamide) (b). Similar to free gluconamide, the [BS]/[B] ratio from the digital integration of Hc (free ABOR) and Hb' (complexed ABOR) signals.

19. Determination of stoichiometry of complex by the Job plot method

Similar to the procedure previously described to determine K_a from ^{1}H NMR spectra (section 3), solutions of the complexes of APBA with saccharides were obtained by mixing various volumes of a stock solution of APBA (2 mM) with a stock solution of saccharide (2 mM) prepared in 0.01 M PBS pH 7.4 (± 0.1). By varying the ratio *r*, which corresponds to [APBA]/([APBA]+[saccharide]), in the range 0.1-0.9, molar concentrations of complex were determined from ^{1}H NMR spectra by digital integration of aryl protons of APBA/saccharide complexes and of free APBA. This allows determination of the stoichiometry of the complexes of APBA with sugars (free gluconamide, free maltose-COOH and HA-maltose) from Job plots obtained from the variation of [BS] (1:1 binding stoichiometry) or [B_2S + BS] (2:1 binding stoichiometry) as a function of *r* (Figure S28).

20. Job plot of the APBA/gluconamide complex

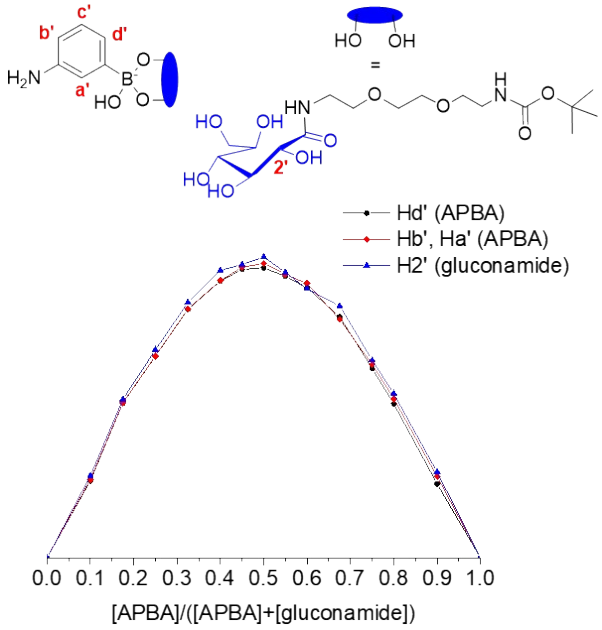

Figure S28. ^{1}H NMR Job plot for APBA and free gluconamide, showing a maximum at a molar ratio of 0.5.

21. Analysis of the binding mode of APBA towards fructose grafted on HA by ^{13}C NMR spectroscopy

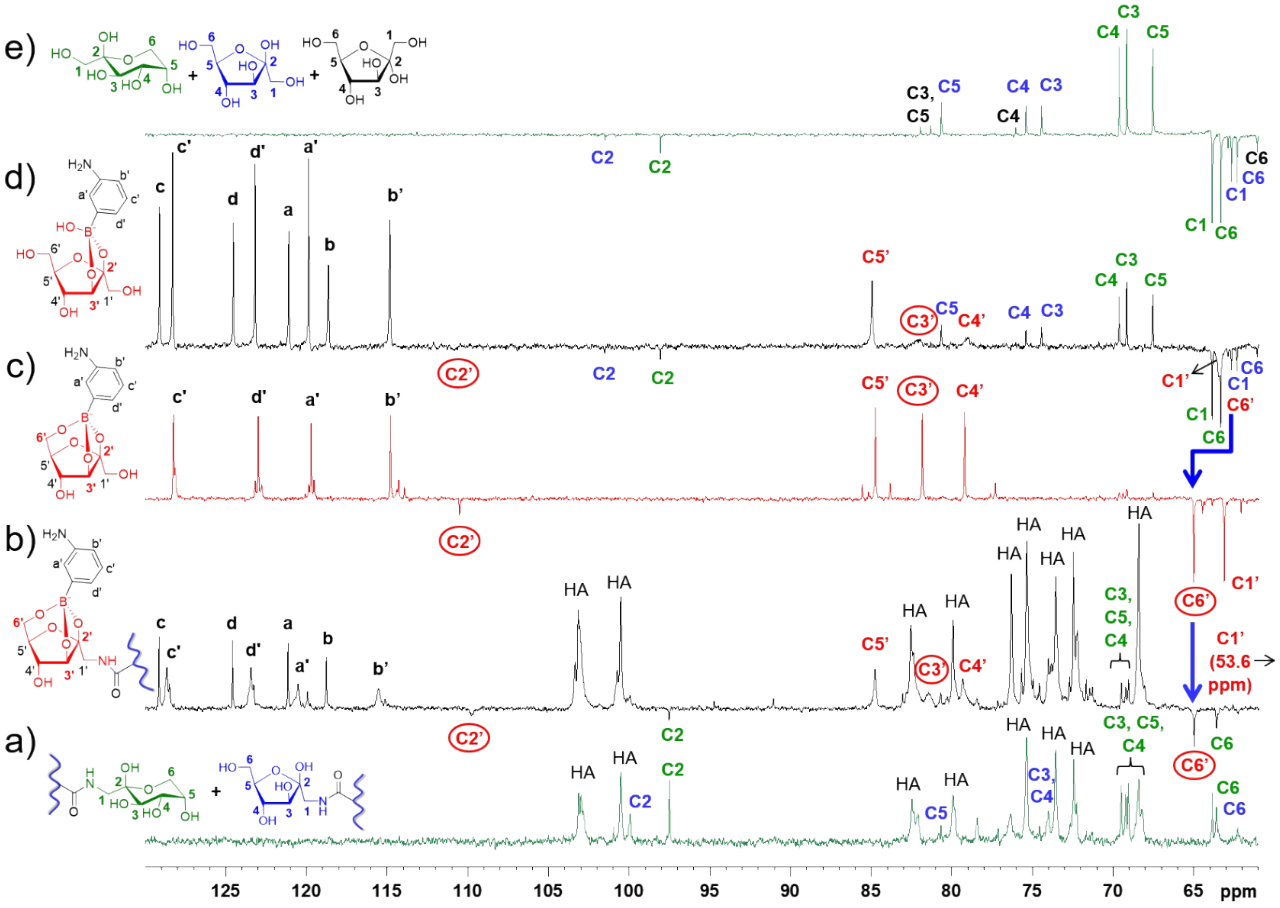

Figure S29. ^{13}C NMR spectrum of HA-fructose alone at pD 7.4 (a), and DEPTQ-135 NMR spectra of APBA/HA-fructose at pD 7.4 (b), APBA/D-fructose at pD 12 (c), APBA/D-fructose at pD 7.4 (d) and D-fructose alone at pD 7.4 (e). Of note, spectrum (a) shows that β-D-fructopyranose (highlighted in green) is the major tautomeric form observed for grafted fructose moieties (HA-fructose), followed by the β-D-fructofuranose form (highlighted in blue); these forms are also observed in the spectrum (e) of D-fructose, in addition to a small fraction of the α-D-fructofuranose form (highlighted in black). In the spectra of APBA/HA-fructose and APBA/D-fructose (spectra (b) and (d), respectively), fructose is partially bound to APBA in the furanose form (highlighted in red), in addition to the unbound β-D-fructofuranose and/or β-D-fructopyranose forms.

22. Evidence of the opening of the endocyclic B-O bond of ABOR bound to free/grafted fructose by ^{1}H NMR spectroscopy

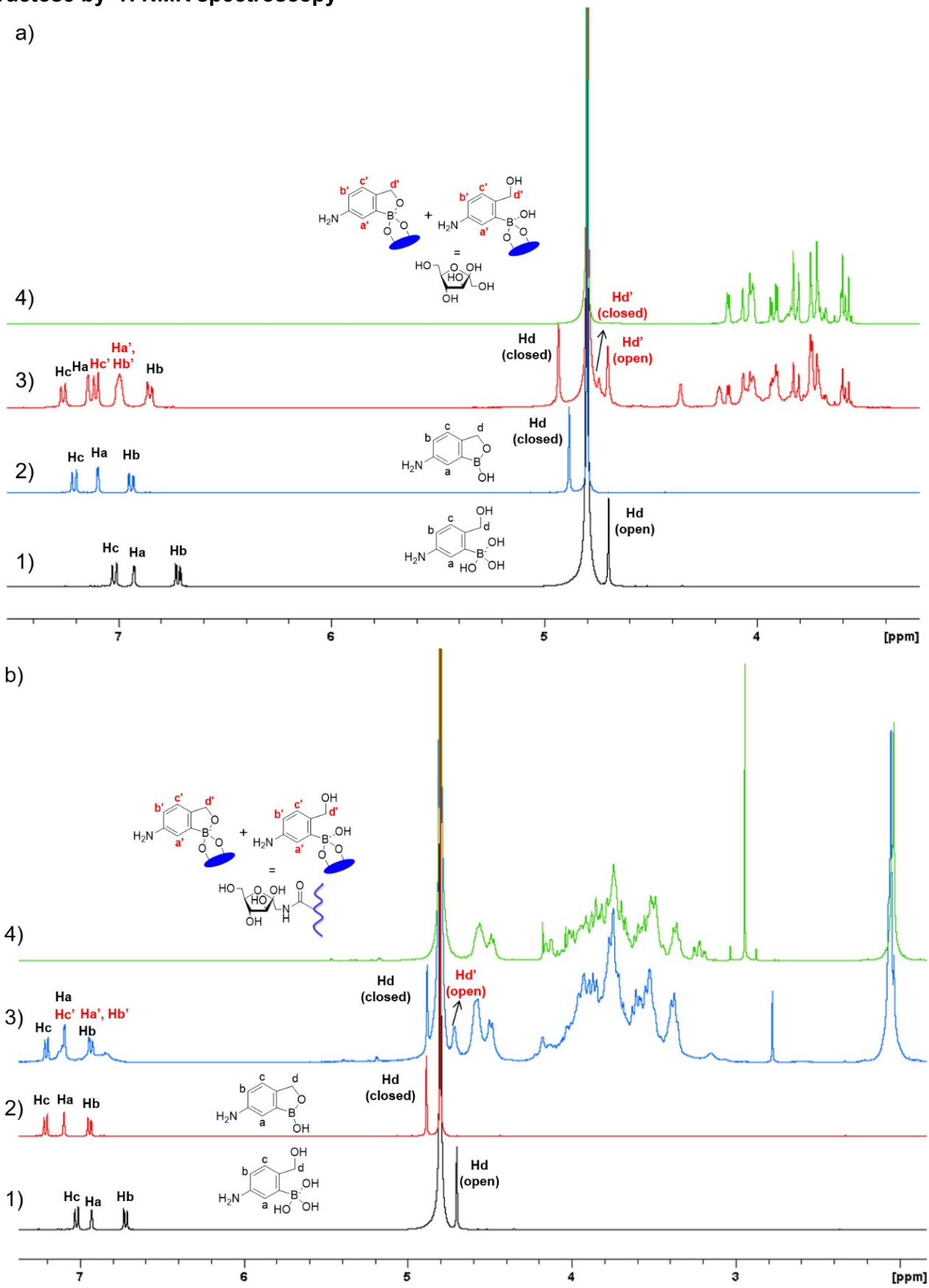

Figure S30. (a) ^{1}H NMR spectra of ABOR alone at pD 11-12 (1), at pD 7.4 (2), ABOR in the presence of D-fructose (3) at pD 7.4 and D-fructose alone (4). (b) ^{1}H NMR spectra of ABOR alone at pD 11-12 (1), at pD 7.4 (2), ABOR in the presence of HA-fructose (3) at pD 7.4 and HA-fructose alone (4) (ABOR/fructose molar ratio of 1:1).

23. Determination of the structure of ABOR complexes with free/grafted fructose by ^{13}C NMR spectroscopy

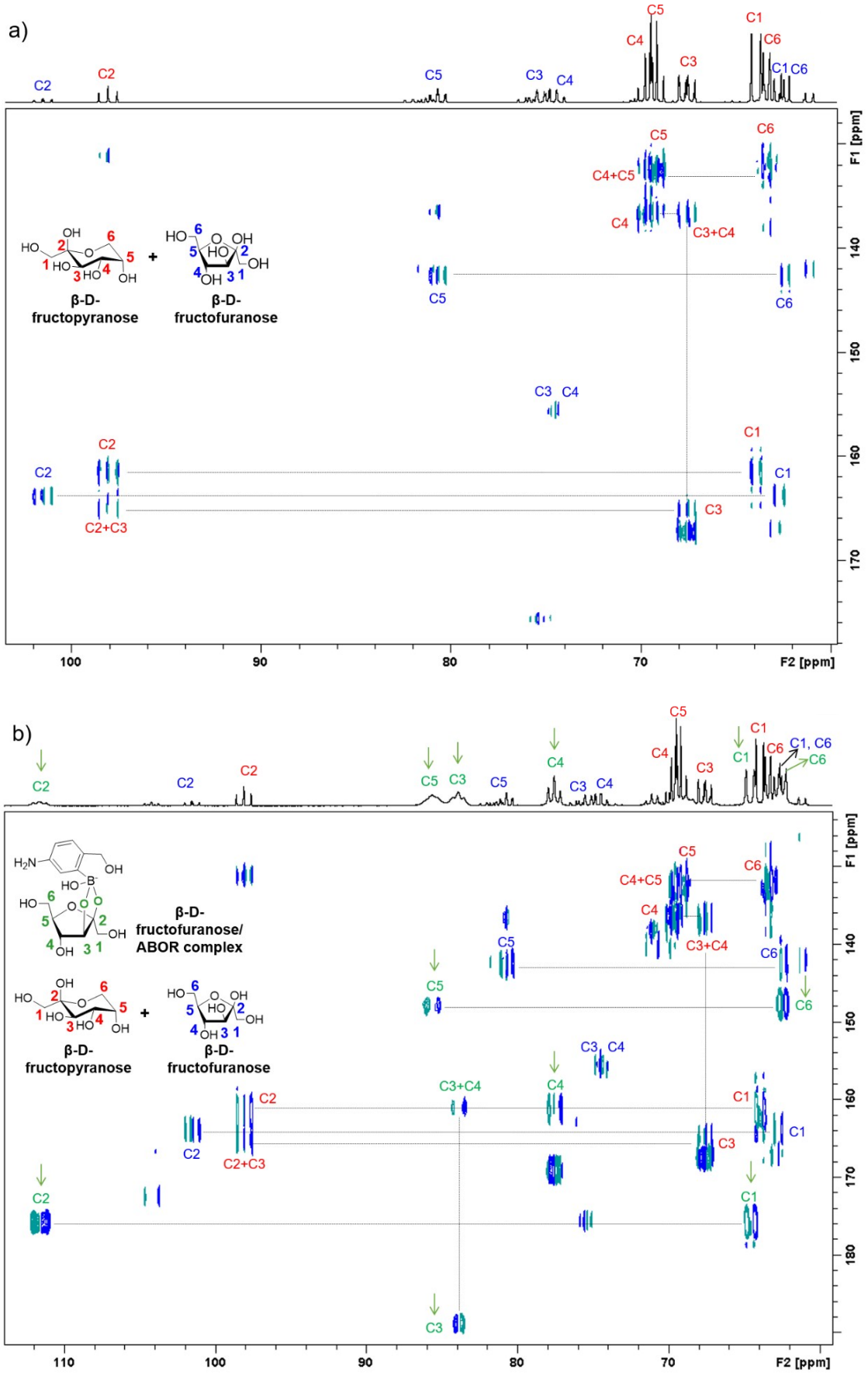

Figure S31. 2D INADEQUATE NMR spectra (400 MHz, D_2O, 298 K) of ^{13}C labeled D-fructose (a) in the absence and (b) in the presence of ABOR at pD 7.4 (ABOR/fructose molar ratio of 1).

24. Determination of the structure of the complex of APBA with a ^{13}C labeled maltose grafted on HA by a ^{13}C-edited HSQC NMR experiment

Table S4. $^{1}H/^{13}C$ chemical shifts (δ in ppm) for grafted ^{13}C labeled maltose (HA-maltose) alone and bound to APBA in D_2O at pD 7.4 (C1-C6: open glucose unit; C1'-C6': terminal glucopyranose unit, see Figure S32).

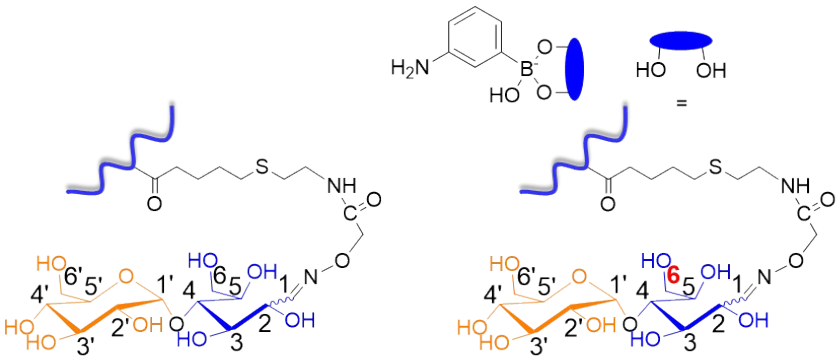

HA-maltose **APBA/HA-maltose**

		δ (ppm)					
Entry	Compound	H1/C1	H2/C2	H3/C3	H4/C4	H5/C5	H6/C6
1	HA-maltose	--[a]	4.6/71.8 *(trans)* 5.1/68.3 *(cis)*	4.05/74.8 *(trans)* 4.0/75.4 *(cis)*	3.9/82.8	--[a]	3.85-3.7/65.6 *(trans)* 3.8-3.7/65.05 *(cis)*
2	APBA/HA-maltose	--[a]	4.6/71.8 *(trans)* 5.1/68.3 *(cis)*	4.05/74.8 *(trans)* 4.0/75.4 *(cis)*	3.9/82.8	--[a]	3.85-3.7/65.6 *(trans)* 3.8-3.7/65.05 *(cis)* **3.8-3.7/65.9[b]**
Entry	Compound	H1'/C1'	H2'/C2'	H3'/C3'	H4'/C4'	H5'/C5'	H6'/C6'
3	HA-maltose	5.15/103.1	3.6/74.4	3.7/75.5	3.4/72.1	3.8/75.5	3.9-3.8//63.15
4	APBA/HA-maltose	5.15/103.1	3.6/74.4	3.8/75.5	3.4/72.1	3.8/75.5	3.9-3.8//63.15

[a]No C1 and C5 signals of the open glucose unit were detected in the ^{13}C-edited HSQC experiments; [b]upshift of the C6 of the open glucose unit in the presence of APBA.

Table S5. $^{1}J_{CC}$ coupling constants (in Hz) for the ^{13}C labeled maltose grafted on HA (HA-maltose) alone and bound to APBA in D_2O at pD 7.4 (C1-C6: open glucose unit; C1'-C6': terminal glucopyranose unit).

Entry	Compound	$^{1}Jc_1$-c_2	$^{1}Jc_2$-c_3	$^{1}Jc_3$-c_4	$^{1}Jc_4$-c_5	$^{1}Jc_5$-c_6
1	HA-maltose	48.3 *(trans)* 42.6 *(cis)*	46.9 *(trans)* 41.3 *(cis)*	47.9 *(trans)* 42.8 *(cis)*	46.0	41.8 *(trans)* 39.9 *(cis)*
2	APBA/HA-maltose	48.5 *(trans)* 42.5 *(cis)*	47.3 *(trans)* 39.1 *(cis)*	46.2 *(trans)* 41.2 *(cis)*	45.0	42.1 *(trans)* 39.1 *(cis)* 42.4[a]
Entry	Compound	$^{1}Jc_{1'}$-$c_{2'}$	$^{1}Jc_{2'}$-$c_{3'}$	$^{1}Jc_{3'}$-$c_{4'}$	$^{1}Jc_{4'}$-$c_{5'}$	$^{1}Jc_{5'}$-$c_{6'}$
3	HA-maltose	46.8	45.0	43.2	38.3	40.5
4	APBA/HA-maltose	47.1	45.8	46.7	37.8	43.4

[a]Upshift of the C6 of the open glucose unit in the presence of APBA.

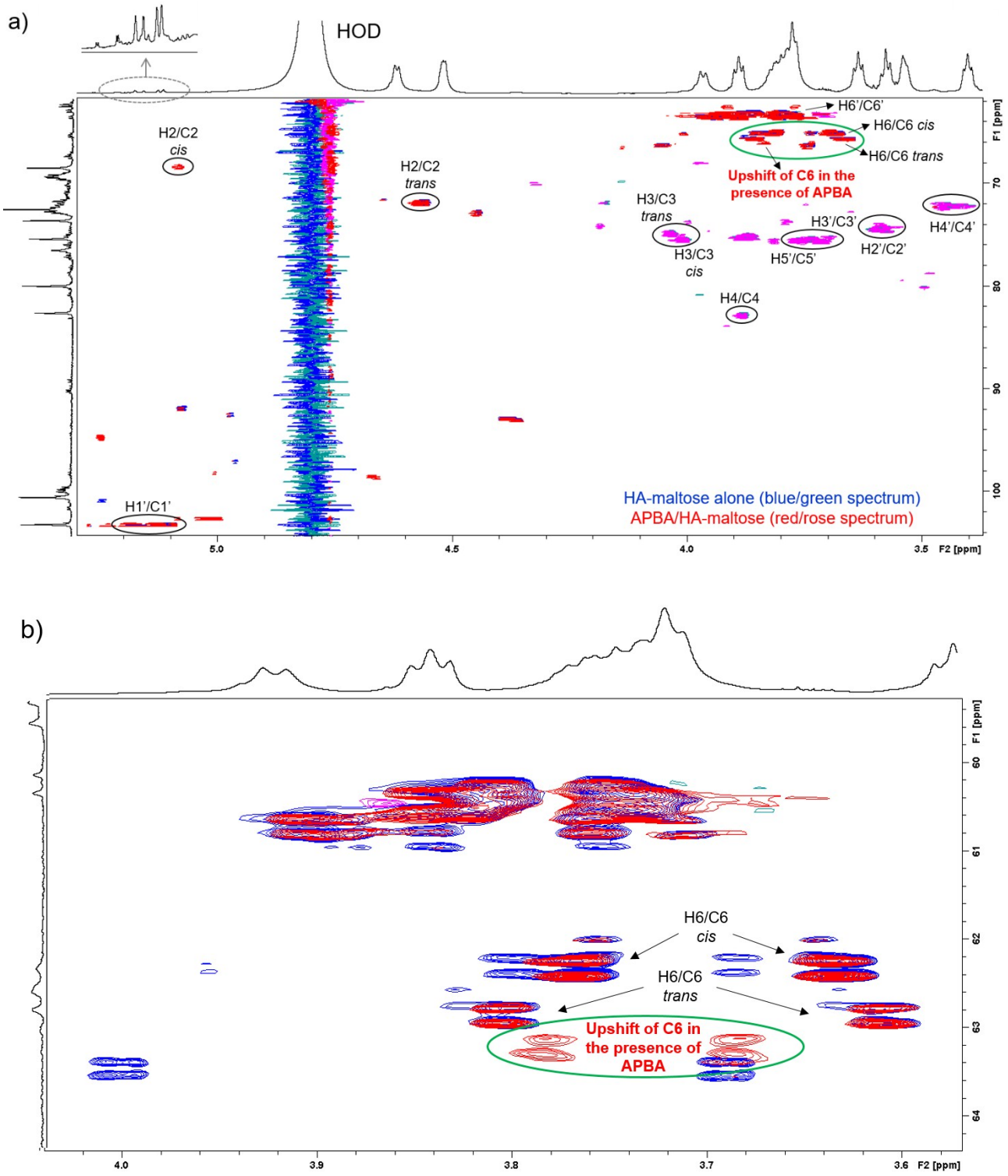

Figure S32. (a) Overlay of the ^{13}C-edited HSQC NMR spectra (950 MHz, D_2O, 298 K) of grafted ^{13}C labeled maltose (HA-maltose) alone (blue/green spectrum) and bound to APBA (red/rose spectrum) in D_2O at pD 7.4 ([APBA]/[grafted maltose] = 1; C1-C6: open glucose unit; C1'-C6': terminal glucopyranose unit). (b) Zoom of the two overlayed spectra in the zone of the C6 and C6' signals. $^1J_{CC}$ coupling constants of the ^{13}C labeled maltose grafted on HA were measured from the cross-peaks of the spectra.

25. Screening of rotamers of the PBA/maltose derivative complexes by classical molecular dynamics with all-atom GROMOS force field performed using GROMACS software

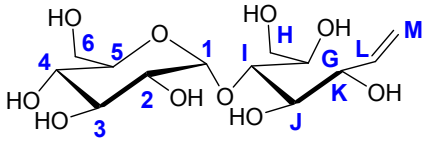

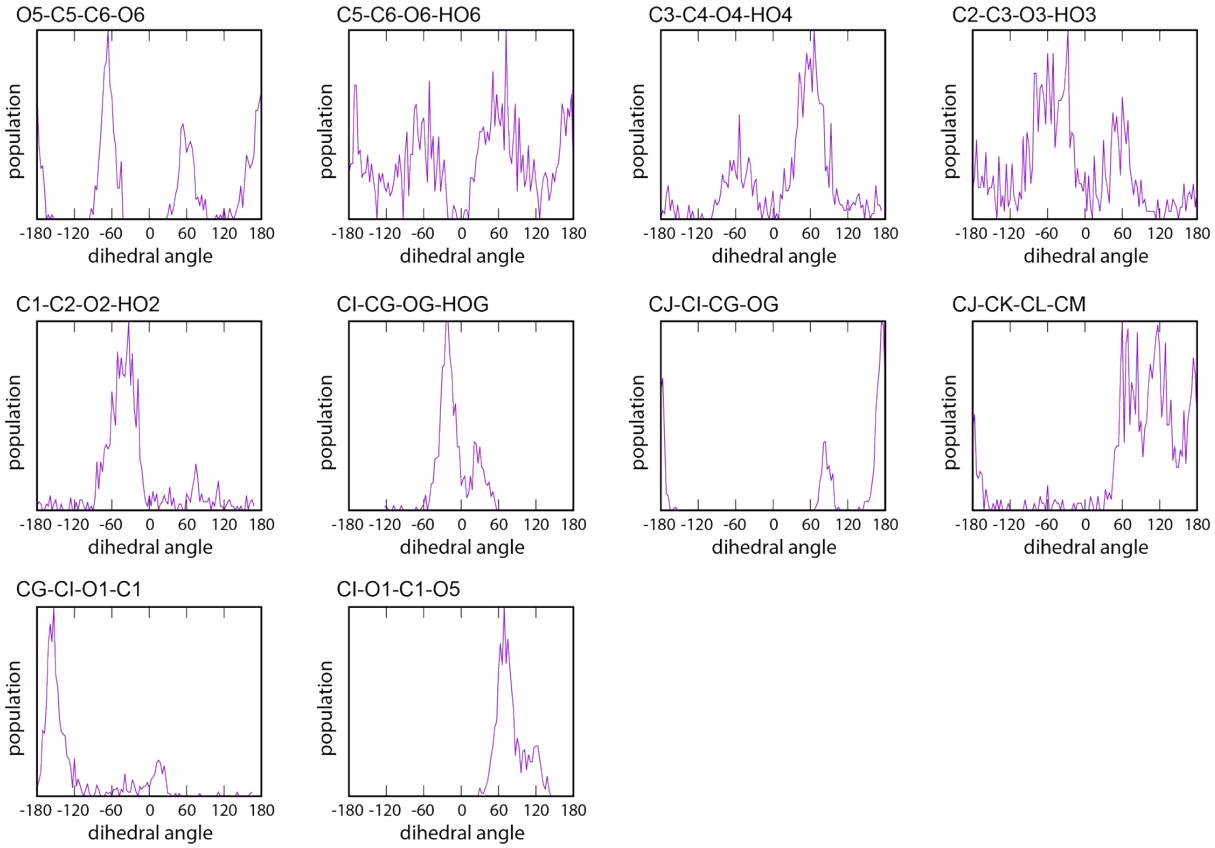

Figure S33. Distributions of selected dihedral angles of complex **1** calculated from MD trajectory.

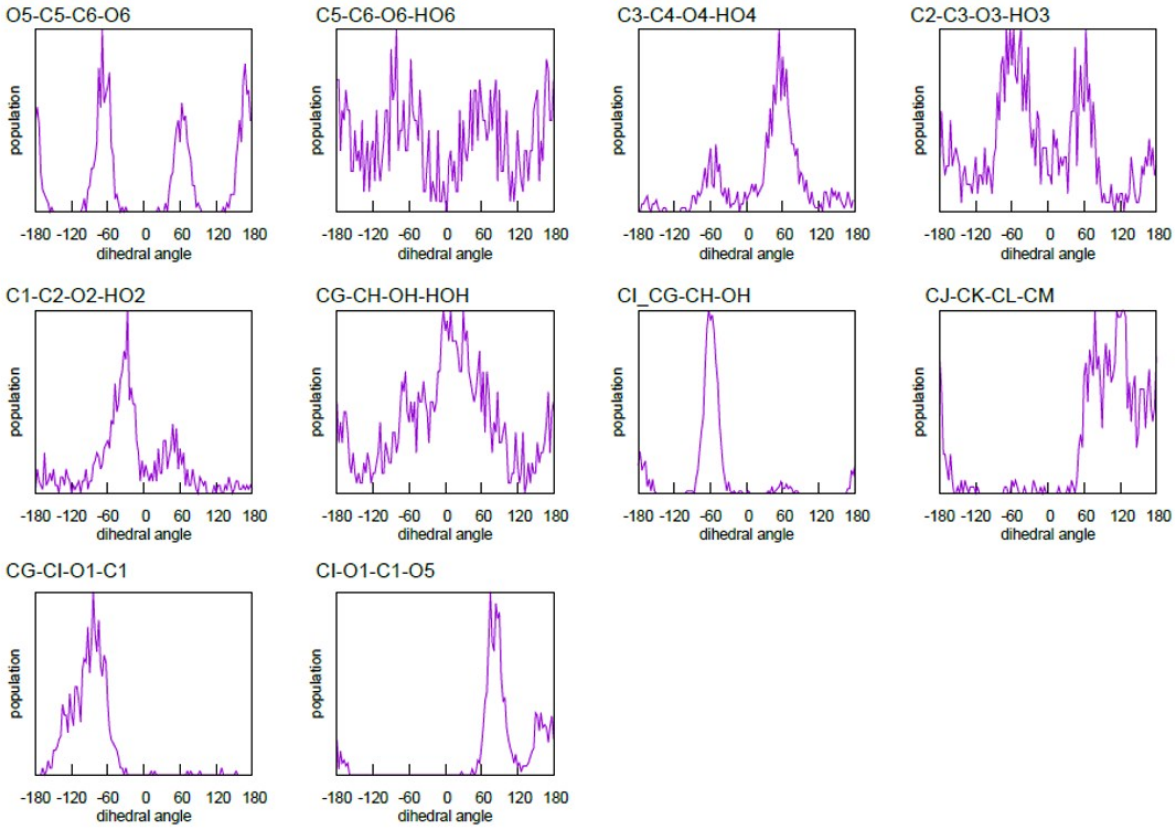

Figure S34. Distributions of selected dihedral angles of complex **2** calculated from MD trajectory.

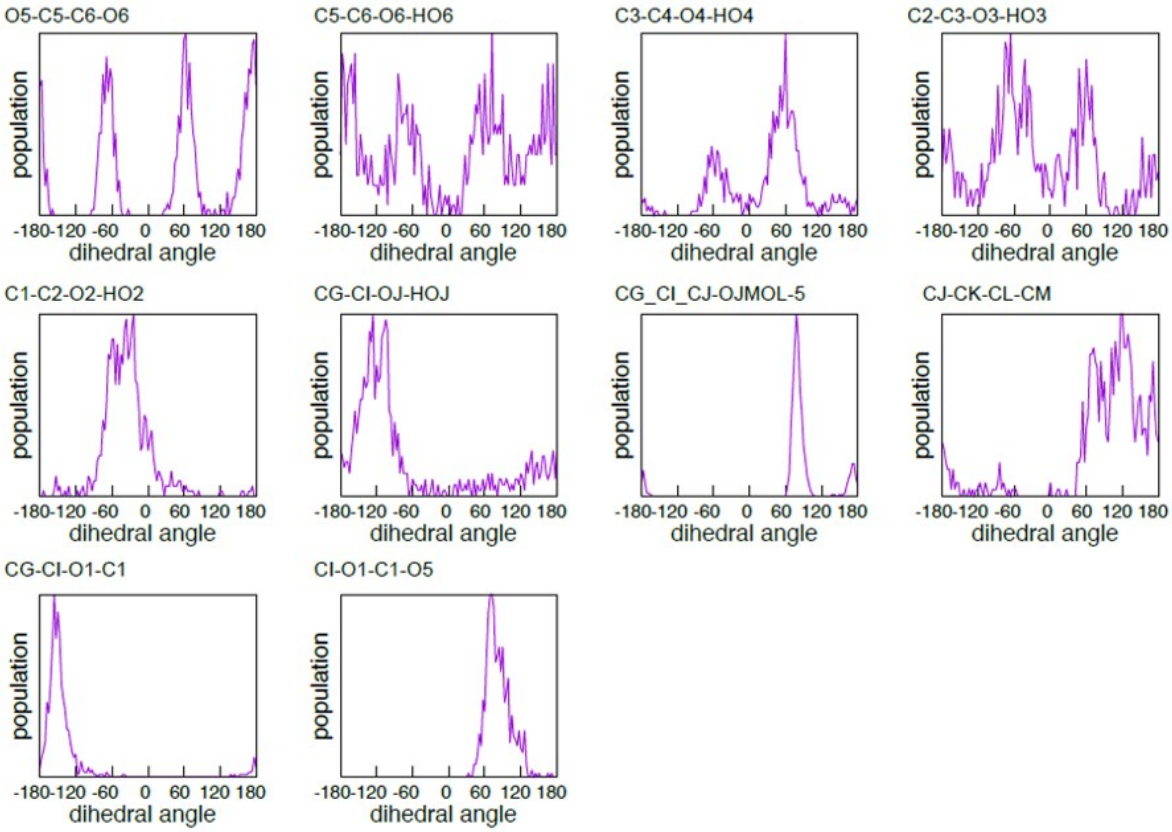

Figure S35. Distributions of selected dihedral angles of complex **3** calculated from MD trajectory.

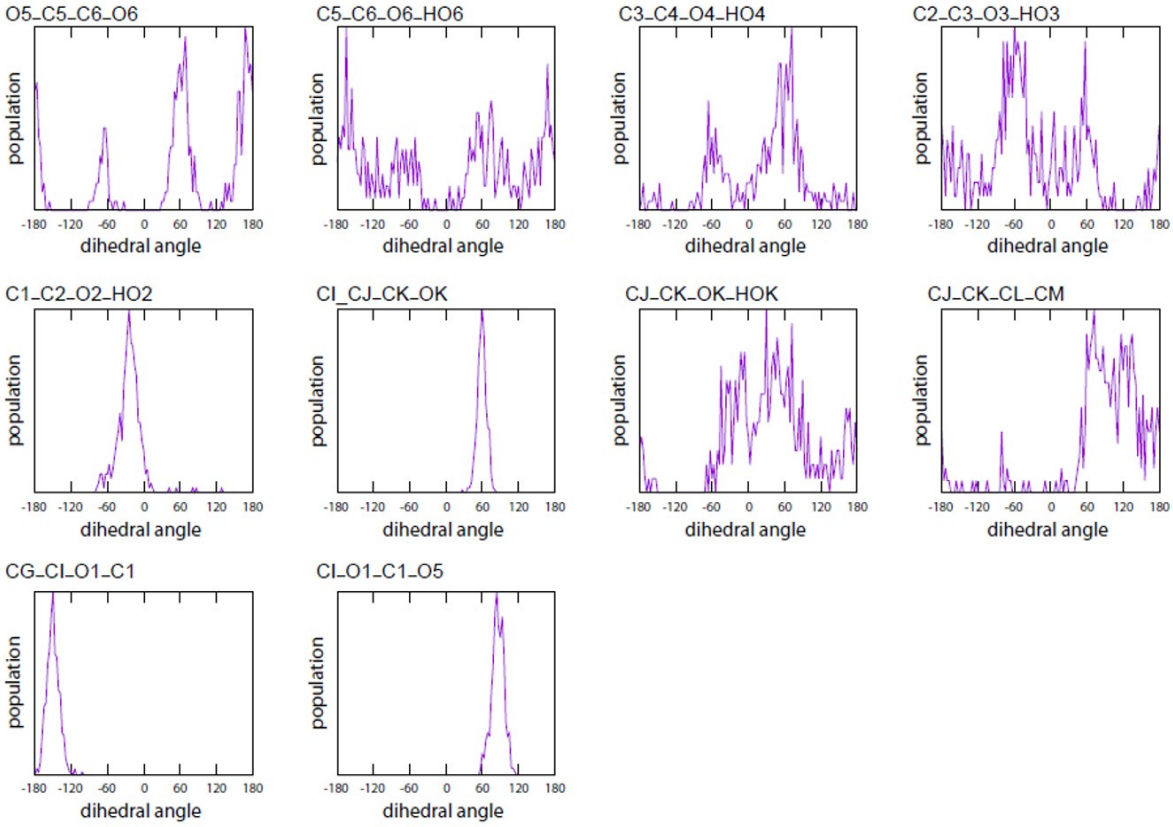

Figure S36. Distributions of selected dihedral angles of complex **4** calculated from MD trajectory.

26. Cartesian coordinates (in Å) of the lower-energy conformers for the complexes of PBA/maltose optimized using M062X/6-311+G(d,p) including SMD in water

Complex 1: C2-OH, C3-OH, C6-OH

C	6.52328900	-0.54778500	0.96422600
H	7.14543400	-0.77270200	1.82424000
C	7.10931300	-0.11567400	-0.22476400
H	8.18546800	-0.00219800	-0.29498700
C	6.29828000	0.16973200	-1.32005700
H	6.74365200	0.50721000	-2.25015200
C	4.91382600	0.02758100	-1.22089600
H	4.29846700	0.26843000	-2.08276400
C	4.29998900	-0.40658700	-0.04028700
C	5.14001100	-0.69204600	1.04661900
H	4.70376000	-1.03054500	1.98316600
B	2.69551400	-0.53902400	0.10694700
O	1.97429800	-0.19574200	-1.14095500
O	2.14306800	0.46333500	1.10927300
O	2.37520800	-1.90065200	0.58256400
C	1.10904600	-2.45772700	0.28768400
H	1.00957600	-3.35808000	0.89990200
H	1.04981500	-2.76298700	-0.76486100
C	-0.08775600	-1.55250700	0.59471500
H	-0.98072400	-2.18568800	0.57927000
O	-0.00766100	-1.02310600	1.91163400
H	0.83887400	-0.54131600	1.96043300
C	-0.33272100	-0.48310700	-0.47776900
H	-0.54634900	-1.03052700	-1.40309600
C	0.80196500	0.50278200	-0.77698000
H	0.47371300	1.14705400	-1.59931200
C	1.23823100	1.32680500	0.45002600
H	0.37863400	1.53501800	1.09877200
C	1.85322600	2.63489200	0.03511500
H	1.15783000	3.33690200	-0.42294900
C	3.13372600	2.95961500	0.17970500
H	3.84156200	2.27561900	0.63692500
H	3.50773200	3.92173800	-0.15310100
O	-1.48690100	0.27228200	-0.09826400
C	-2.42006900	0.48319600	-1.11897200
H	-1.91963700	0.64678600	-2.07677800
C	-3.24902600	1.70304600	-0.72585800
H	-3.89890800	1.95997800	-1.56556100
O	-2.41140100	2.82274600	-0.49791800
H	-1.71484100	2.54511500	0.11431600
C	-4.11284200	1.38782900	0.49074000
H	-3.46778100	1.21721300	1.36228600
O	-5.02168300	2.44437300	0.76462600
H	-4.51400900	3.21681100	1.04070300
C	-4.93540200	0.13313700	0.24028300
H	-5.63988900	0.32768000	-0.57995100
O	-5.63748700	-0.25842500	1.40896800
H	-6.14872000	0.50153300	1.71322400
C	-4.01087700	-1.01402100	-0.15312900
H	-3.33192300	-1.23639300	0.67888800
O	-3.24909800	-0.64363400	-1.30719700
C	-4.76695300	-2.26829000	-0.53530300
H	-5.41009600	-2.05570700	-1.39688000
H	-5.38887900	-2.58979800	0.29944900
O	-3.87526600	-3.33602800	-0.82693800
H	-3.30647000	-3.05244100	-1.55285100

Complex 2: C2-OH, C3-OH, C5-OH

C	-6.33868000	-1.75770900	-0.32336100
H	-6.76986200	-2.72441800	-0.56091700
C	-7.16675200	-0.69676600	0.03221400
H	-8.24188800	-0.83221300	0.07157500
C	-6.60208800	0.54092700	0.33724000
H	-7.23909800	1.37378800	0.61535100
C	-5.22050400	0.70580400	0.28039800
H	-4.79427300	1.67844400	0.51443600
C	-4.36438900	-0.34578500	-0.07694100
C	-4.95578700	-1.57855100	-0.37489500
H	-4.32814300	-2.41875100	-0.65569700
B	-2.77820200	-0.08718900	-0.12041800
O	-2.22237200	0.29118500	1.21570100
O	-2.41044600	1.10044500	-0.95994900
O	-2.05220700	-1.28770500	-0.60681600
C	-0.02530500	-2.47844900	-0.90338100
H	1.06303400	-2.39893900	-0.93018400
H	-0.36820800	-2.92811100	-1.84147200
O	-0.36074100	-3.32137800	0.19385700
H	-1.31523400	-3.23617800	0.31908300
C	-0.65644800	-1.10432600	-0.75525200
H	-0.44010300	-0.52946000	-1.66743800
C	-0.05975100	-0.32670400	0.42838100
H	0.07290000	-0.99902800	1.28288600
C	-0.96709500	0.83225600	0.85135700
H	-0.51351000	1.38010800	1.68272100
C	-1.30114300	1.74958200	-0.34646000
H	-0.45577500	1.80355100	-1.04367900
C	-1.66518500	3.13488200	0.09904000
H	-2.54036200	3.20805800	0.74396900
C	-0.97351900	4.22026500	-0.23282700
H	-0.10367600	4.15361000	-0.88161500
H	-1.24885100	5.20497400	0.12902400
O	1.20977300	0.17848100	0.00909300
C	2.17975100	0.27168200	1.01713000
H	1.71075700	0.37911000	1.99753600
C	3.05300400	1.48758700	0.71000200
H	3.72628300	1.64744900	1.55569300
O	2.26130200	2.65663900	0.59474900
H	1.56448600	2.47811400	-0.05348700
C	3.88555300	1.24389600	-0.54222500
H	3.22212200	1.16173000	-1.41313800
O	4.82392400	2.29005600	-0.74949900
H	4.33648500	3.10140200	-0.93542300
C	4.66720400	-0.04957900	-0.39225800
H	5.37417900	0.05801100	0.43953500
O	5.36082800	-0.37138400	-1.58735900
H	5.92860000	0.37700400	-1.80780100
C	3.70505300	-1.19611300	-0.09724000
H	3.02507100	-1.31336900	-0.94923200
O	2.95561000	-0.90496400	1.08806000
C	4.39833000	-2.52140800	0.14399600
H	4.94818000	-2.81035900	-0.75151600
H	3.63729900	-3.28207500	0.34546700
O	5.33802600	-2.45993000	1.20812200
H	4.85752200	-2.25702600	2.01924500

Complex 3: C2-OH, C5-OH, C6-OH

C	5.66247700	-0.84945700	2.03176200
H	6.18931600	-0.34198700	2.83311400
C	6.07018400	-2.11692200	1.62671300
H	6.91247100	-2.60114600	2.10834500
C	5.38598800	-2.75916200	0.59488200
H	5.69767000	-3.74647200	0.27098400
C	4.30565600	-2.12973000	-0.01795200
H	3.78432300	-2.64321700	-0.82277700
C	3.87223700	-0.85329000	0.37086800
C	4.57738300	-0.23147500	1.40777200
H	4.27661600	0.75855000	1.73666900
B	2.58726500	-0.19083300	-0.35830200
O	1.32162900	-0.87634800	0.02469200
O	2.63960500	-0.38866200	-1.85974000
O	2.53918900	1.25332500	-0.06624900
C	1.51921600	-1.16660000	-2.25463000
H	1.78611100	-2.22834000	-2.30481600
H	1.15536800	-0.84605400	-3.23454400
C	0.50782400	-0.94089500	-1.13430700
H	-0.19627200	-1.77329500	-1.04522100
C	-0.31634600	0.33309300	-1.31651900
H	-0.85915500	0.25296000	-2.26569500
C	0.44400600	1.67330900	-1.30558000
H	-0.33106700	2.44617000	-1.32364400
O	1.22075000	1.86056800	-2.47672900
H	1.96362400	1.22889400	-2.41712900
C	1.29354000	1.90466400	-0.03079200
H	0.69548600	1.53460700	0.81498700
C	1.48132300	3.38348900	0.16839200
H	0.55357600	3.93919300	0.29280100
C	2.64550300	4.02326000	0.19591700
H	3.58694100	3.49812600	0.07864500
H	2.68530700	5.09694800	0.34301500
O	-1.25711000	0.37948900	-0.23478000
C	-2.53763000	0.83516700	-0.57293300
H	-2.48709300	1.60943300	-1.34282900
C	-3.17039100	1.38262300	0.70387200
H	-4.12494800	1.84649500	0.44404500
O	-2.36135000	2.39913600	1.26762000
H	-1.46577600	2.04223000	1.35303300
C	-3.42203400	0.24907200	1.69043100
H	-2.46304400	-0.17766400	2.01105300
O	-4.14858200	0.70363200	2.82337600
H	-3.59334000	1.32753600	3.30594000
C	-4.24801600	-0.83548900	1.02164300
H	-5.23006500	-0.41939000	0.76413200
O	-4.39905700	-1.96255600	1.87018500
H	-4.78421500	-1.65591000	2.70007200
C	-3.54963000	-1.31005900	-0.25049300
H	-2.59111100	-1.77014500	0.01866500
O	-3.32655900	-0.19771900	-1.12457300
C	-4.35999100	-2.31951900	-1.03793400
H	-4.53319800	-3.20267400	-0.42332200
H	-3.78649000	-2.61612700	-1.92151100
O	-5.63485600	-1.81878200	-1.41662400
H	-5.49444600	-1.05369000	-1.98660100

Complex 4: C3-OH, C5-OH, C6-OH

C	4.60569500	-1.20471100	2.37490000
H	4.83018400	-0.76343700	3.34017900
C	5.24722600	-2.37567000	1.97982900
H	5.97291600	-2.84841100	2.63232800
C	4.94988500	-2.93465900	0.73823800
H	5.44594300	-3.84617700	0.42202500
C	4.01740000	-2.32061700	-0.09528800
H	3.79850600	-2.76911000	-1.06078800
C	3.35924100	-1.14042000	0.27725000
C	3.67519400	-0.60006900	1.52997100
H	3.18462500	0.31270900	1.85494100
B	2.25974400	-0.48175800	-0.69321900
O	1.97129500	0.92224900	-0.27232700
O	0.97368800	-1.24098200	-0.70236000
O	2.64731100	-0.49426500	-2.13671300
C	1.46124100	-0.70523000	-2.89558300
H	1.33325500	0.07945800	-3.64876400
H	1.50699200	-1.67431600	-3.40340900
C	0.33580200	-0.70295800	-1.85181800
H	-0.52059200	-1.31722000	-2.14014800
C	-0.12379600	0.72288800	-1.52432800
H	-0.62079800	1.17211100	-2.39164100
C	1.08107900	1.59447400	-1.13955600
H	1.59192400	1.85156000	-2.07697200
C	0.67511000	2.91256800	-0.45112100
C	1.75663700	3.94497600	-0.63425800
H	1.95472000	4.21424900	-1.66968300
C	2.45722700	4.50067200	0.34772200
H	2.27651800	4.24896400	1.38727100
H	3.23314300	5.22801700	0.13691700
O	-1.03414700	0.68429900	-0.42539900
C	-2.38790400	0.85229300	-0.71274400
H	-2.52860100	1.58712500	-1.50983200
C	-3.04461700	1.31826300	0.58456900
H	-4.08859800	1.56423900	0.37330800
O	-2.42603600	2.49525000	1.06687400
H	-1.45621300	2.37264900	1.05131000
C	-3.00283300	0.19721900	1.61665700
H	-1.95993600	-0.01001300	1.88849000
O	-3.74269200	0.54337000	2.77996900
H	-3.32192200	1.31225800	3.18292500
C	-3.62290500	-1.06166000	1.03573200
H	-4.68226900	-0.86756300	0.82665500
O	-3.49167800	-2.15969800	1.92535800
H	-3.89984100	-1.91070700	2.76338800
C	-2.91320800	-1.43503400	-0.26414000
H	-1.86314400	-1.66662700	-0.04577300
O	-2.98664700	-0.33962600	-1.18268900
C	-3.52731400	-2.62959000	-0.96457100
H	-3.46663200	-3.50149800	-0.31343300
H	-2.95413300	-2.83489300	-1.87436900
O	-4.90118700	-2.43700900	-1.27364700
H	-4.96920100	-1.68384000	-1.87210800
O	0.38782700	2.69077000	0.92331800
H	0.97506500	1.97160800	1.20420200
H	-0.24745900	3.27638700	-0.91876700

27. Lower-energy conformers for the complexes of PBA/gluconamide complexes obtained by DFT (M062X/6-311+(d,p) in water, SMD)

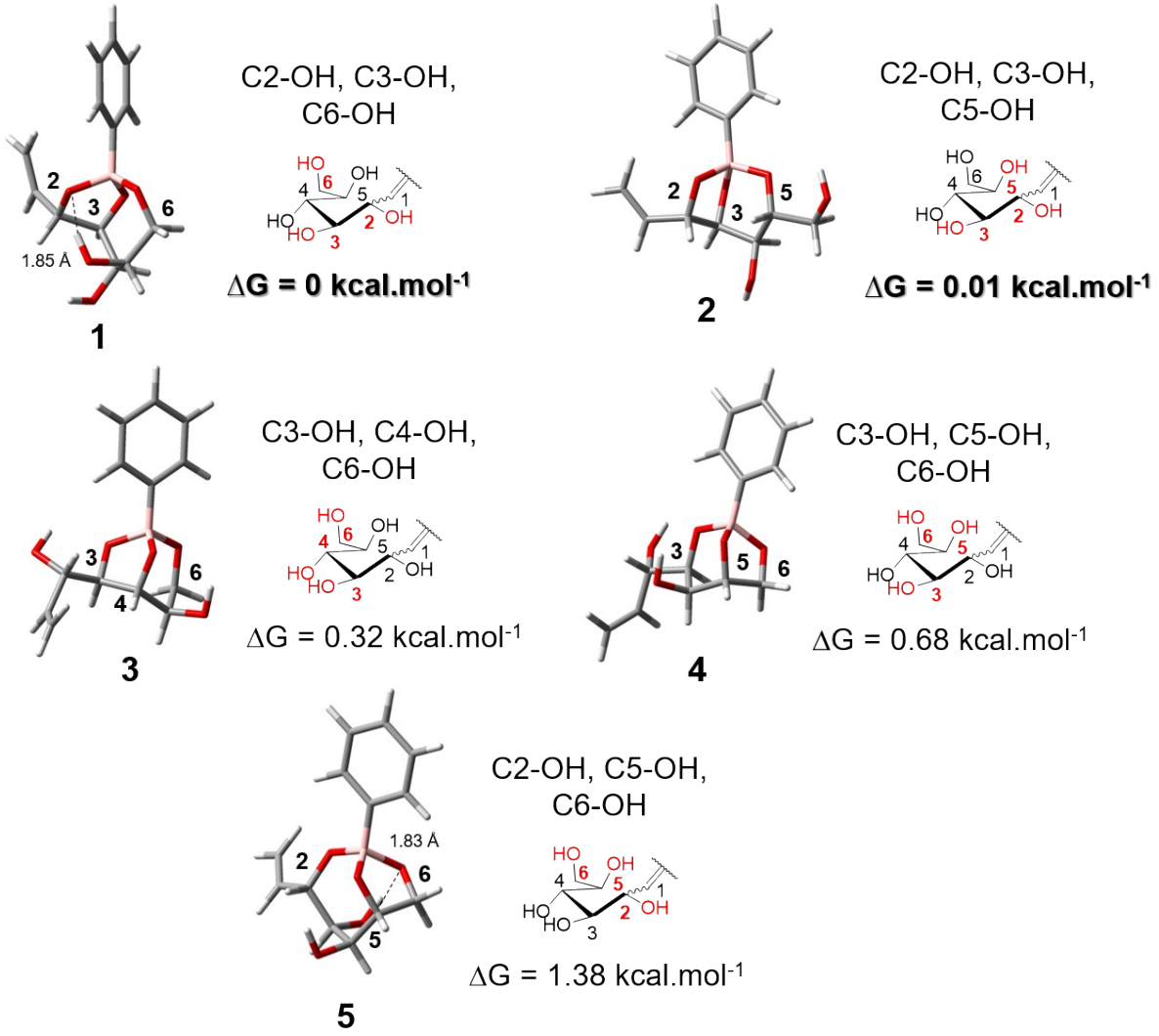

Figure S37. Optimized structures (M062X/6-311+G(d,p)/SMD) of most stable complexes between PBA and gluconamide. Note: The indicated values of energy are relative ones, with the minima set at 0 kcal/mol for the respective lowest energy structures of complex **1**.

28. Cartesian coordinates (in Å) of the lower-energy conformers for the complexes of PBA/gluconamide optimized using M062X/6-311+G(d,p) including SMD in water

Complex 1: C2-OH, C3-OH, C6-OH

C	-3.92674300	-0.88617200	-0.97257200
C	-4.62097600	-0.33343600	0.10269900
C	-3.90870700	0.17465900	1.18561100
C	-2.51400600	0.13179200	1.18704400
C	-1.79213000	-0.41992900	0.12231800
C	-2.53436100	-0.92876200	-0.95399200
B	-0.17566800	-0.45544500	0.08856200
O	0.44000600	0.18253100	1.27432800
O	0.37937000	0.35998900	-1.07022800
O	0.26154300	-1.85597000	-0.08278400
C	1.53438600	-2.23796400	0.40074200
C	2.69285400	-1.32170400	-0.00059000
O	2.69273500	-1.06268500	-1.40205200
C	2.80715500	-0.02679900	0.81855800
C	1.57967300	0.89645700	0.83668000
C	1.15686900	1.41948800	-0.55014900
C	0.40173700	2.71527100	-0.43060400
C	-0.88088900	2.88777800	-0.73224600
O	3.96221100	0.69947900	0.40701600
H	-4.47193700	-1.28227300	-1.82286600
H	-5.70470300	-0.29924900	0.09498900
H	-4.43908900	0.60780900	2.02722900
H	-1.97721900	0.54407500	2.03635500
H	-2.01286000	-1.36374100	-1.80298500
H	1.74189500	-3.23086600	-0.00774500
H	1.53090200	-2.32278800	1.49492500
H	3.61536200	-1.87500600	0.19960100
H	1.81850800	-0.67858100	-1.60451800
H	2.98725400	-0.32939800	1.85431700
H	1.79447100	1.71816100	1.52595800
H	2.02982300	1.58823000	-1.19288100
H	0.99132100	3.55074000	-0.05688500
H	-1.48852500	2.07178200	-1.10980100
H	-1.35733700	3.85463500	-0.61066700
H	3.96436700	0.71286700	-0.55906100

Complex 2: C2-OH, C3-OH, C5-OH

C	-4.58520100	-0.87981700	0.13433400
C	-3.68933700	-1.89218400	-0.19788800
C	-2.31749400	-1.63684600	-0.20558800
C	-1.80359200	-0.37419300	0.11261200
C	-2.72755400	0.62779500	0.44391600
C	-4.09916500	0.38592400	0.45852900
B	-0.23301400	-0.03104400	0.07527000
O	0.22141200	0.74698300	1.26773900
O	0.12943300	0.88973500	-1.05510000
C	1.47005300	1.24069400	0.82043900
C	1.14773700	1.76145600	-0.60164000
C	0.71207700	3.19919400	-0.56765100
C	-0.51557500	3.63407600	-0.83269400
O	0.58190300	-1.26814300	-0.01799400
C	2.45685000	0.06566600	0.79406500
C	1.96931200	-1.02531600	-0.16659300
C	2.69786000	-2.33414400	0.06738400
O	2.27352800	-3.32761700	-0.86105400
H	-5.65195000	-1.07414100	0.14183300
H	-4.05899100	-2.88012300	-0.45107300
H	-1.63563900	-2.44081400	-0.46562900
H	-2.36434000	1.62057600	0.69729900
H	-4.78933300	1.18083500	0.72021600
H	1.84612000	2.02670200	1.48198400
H	2.03695100	1.67864500	-1.24032300
H	1.49229500	3.90477200	-0.28730100
H	-1.30668000	2.94992000	-1.12060700
H	-0.75920800	4.68941300	-0.77730100
H	2.17896400	-0.68432800	-1.19178400
H	2.50978400	-2.67169700	1.09379200
H	3.77184200	-2.20488700	-0.07179000
H	1.30912400	-3.34859300	-0.82337000
O	3.75008800	0.46746500	0.35717500
H	4.12662300	1.05140000	1.02572300
H	2.51276100	-0.34367700	1.81050800

Complex 3: C3-OH, C4-OH, C6-OH

O	0.26037500	0.58513800	1.02628500
C	0.66268500	2.48369600	-1.07405300
H	1.03964100	2.03866200	-2.00370400
H	0.57002900	3.56139300	-1.23161200
C	1.63736600	-0.22464100	-0.64703900
H	2.32661500	0.10006000	-1.43691700
C	1.57526300	0.77303200	0.51820600
H	2.31664500	0.57252700	1.29610400
C	1.67657200	2.22623800	0.04192100
H	2.68330400	2.44456200	-0.32133100
O	-0.61949800	1.95838700	-0.76096200
O	0.30774300	-0.26199000	-1.14353700
B	-0.55042700	0.57762000	-0.23345900
C	-2.01423500	-0.04835300	-0.01583700
C	-3.18477100	0.71844200	-0.05190500
C	-2.15214400	-1.41859400	0.24803100
C	-4.43940500	0.14800000	0.16438000
H	-3.11887000	1.78309400	-0.25413600
C	-3.39847300	-2.00125000	0.46535800
H	-1.26258200	-2.04428400	0.27770300
C	-4.54943600	-1.21545700	0.42356400
H	-5.33051300	0.76596300	0.13179500
H	-3.47580500	-3.06469000	0.66496400
H	-5.52283600	-1.66361000	0.59021100
C	2.03207200	-1.62999400	-0.17084500
H	1.50182200	-1.84064600	0.76697700
O	1.64216400	-2.57994800	-1.16303500
H	0.76766000	-2.29241500	-1.46393300
C	3.50952600	-1.74479100	0.03945200
C	4.07734400	-1.87214000	1.23363400
H	4.11718500	-1.69088500	-0.86234800
H	5.15498100	-1.91600500	1.34713100
H	3.47820800	-1.93043700	2.13800700
O	1.44446700	3.09124500	1.15451200

H	0.63045700	2.78081900	1.57307300

Complex 4: C3-OH, C5-OH, C6-OH

C	-4.62773500	0.25065000	0.09578100
H	-5.47028100	0.93311500	0.06276800
C	-4.84376400	-1.11229100	0.29451500
H	-5.85144500	-1.49405300	0.41574300
C	-3.75558000	-1.97945300	0.33452500
H	-3.91562900	-3.04131300	0.48861800
C	-2.46099700	-1.48273400	0.17871500
H	-1.62493400	-2.17451000	0.21303800
C	-2.21643100	-0.11911400	-0.02188300
C	-3.33003800	0.73248500	-0.05929100
H	-3.17790200	1.79760400	-0.21534300
B	-0.73767700	0.48963900	-0.19385300
O	0.28577200	-0.59090300	-0.14175700
O	-0.40298100	1.50055200	0.85749100
O	-0.56727900	1.27981400	-1.45445300
C	0.31867600	2.35635500	-1.16783200
H	1.17380400	2.35580500	-1.85219700
H	-0.20722800	3.31186900	-1.26566200
C	0.74073800	2.12897700	0.28791600
H	0.97025600	3.05537200	0.81856300
C	1.91163500	1.14631800	0.42065600
C	1.60328300	-0.12687900	-0.38287800
H	1.71683900	0.11906900	-1.44952000
C	2.55114800	-1.28512500	-0.07354800
C	3.96595000	-0.96959000	-0.45109200
H	4.14507800	-0.78348700	-1.50880100
C	4.95758500	-0.89414500	0.42934100
H	4.78555500	-1.08160800	1.48544700
H	5.96747700	-0.64024600	0.12624600
H	2.49394900	-1.51597300	0.99525300
O	2.13065600	-2.42702600	-0.82775400
H	1.16524700	-2.44464700	-0.76478500
H	2.83403500	1.59600500	0.04688000
O	2.12150600	0.86807600	1.80330400
H	1.25534600	0.64198900	2.16881600

Complex 5: C2-OH, C5-OH, C6-OH

C	3.91651000	1.38780900	0.47630300
C	4.75505100	0.30622500	0.22361200
C	4.19929800	-0.92238300	-0.13279900
C	2.81712000	-1.05520400	-0.23243100
C	1.94807500	0.01770300	0.01824900
C	2.53208300	1.23845900	0.37375700
B	0.34972100	-0.21684500	-0.09808400
O	-0.14066500	-1.15787000	0.94797200
O	-0.01106200	-0.92284000	-1.39116900
O	-0.34796300	1.07757000	-0.05219400
C	-0.59948500	-2.17548400	-1.07390000
C	-1.12509700	-1.98408300	0.34342300
C	-2.49848800	-1.31680500	0.42566300
C	-2.62173200	0.10331700	-0.16888600
O	-2.52515300	0.10183900	-1.58522100
C	-1.66197700	1.15224600	0.44442400
C	-2.22197800	2.52913800	0.20544500
C	-1.60394700	3.51351100	-0.43823800
O	-2.90863400	-1.27215300	1.79278200
H	4.33984000	2.34760000	0.75318700
H	5.83097000	0.41786300	0.30113600
H	4.84500500	-1.77062000	-0.33440100
H	2.39958000	-2.01892200	-0.51569400
H	1.89492400	2.09434800	0.57485200
H	0.15601000	-2.96949900	-1.08629800
H	-1.38471800	-2.42433100	-1.79297400
H	-1.18847900	-2.93354300	0.88279400
H	-3.22513500	-1.94983900	-0.09198600
H	-3.64000600	0.42039000	0.07178300
H	-1.59104100	-0.09268000	-1.79610000
H	-1.66684800	0.99049600	1.53319600
H	-3.21918900	2.68828000	0.61089200
H	-0.60808900	3.38640200	-0.84820700
H	-2.08055000	4.47907800	-0.56813500
H	-2.15564000	-0.95984800	2.31128000

29. Possible structures of binding modes for BOR with the maltose derivative grafted on HA

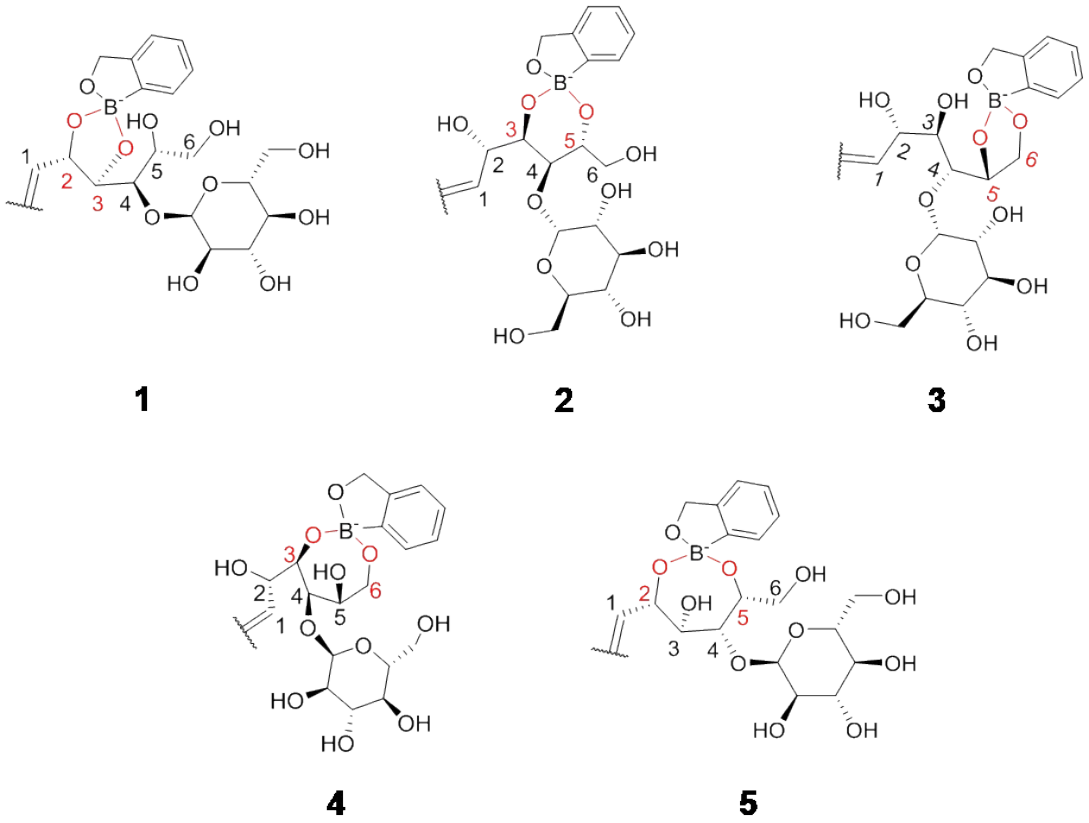

Figure S38. Possible binding modes of BOR with grafted maltose. These structures illustrate possible complexes based on the most favorable complexes found for PBA/maltose from DFT calculations, without considering possible complexation of OH groups from the glycopyranoside unit.

30. Evidence of the cyclic structure of ABOR bound to free/grafted maltose by ^{1}H NMR spectroscopy

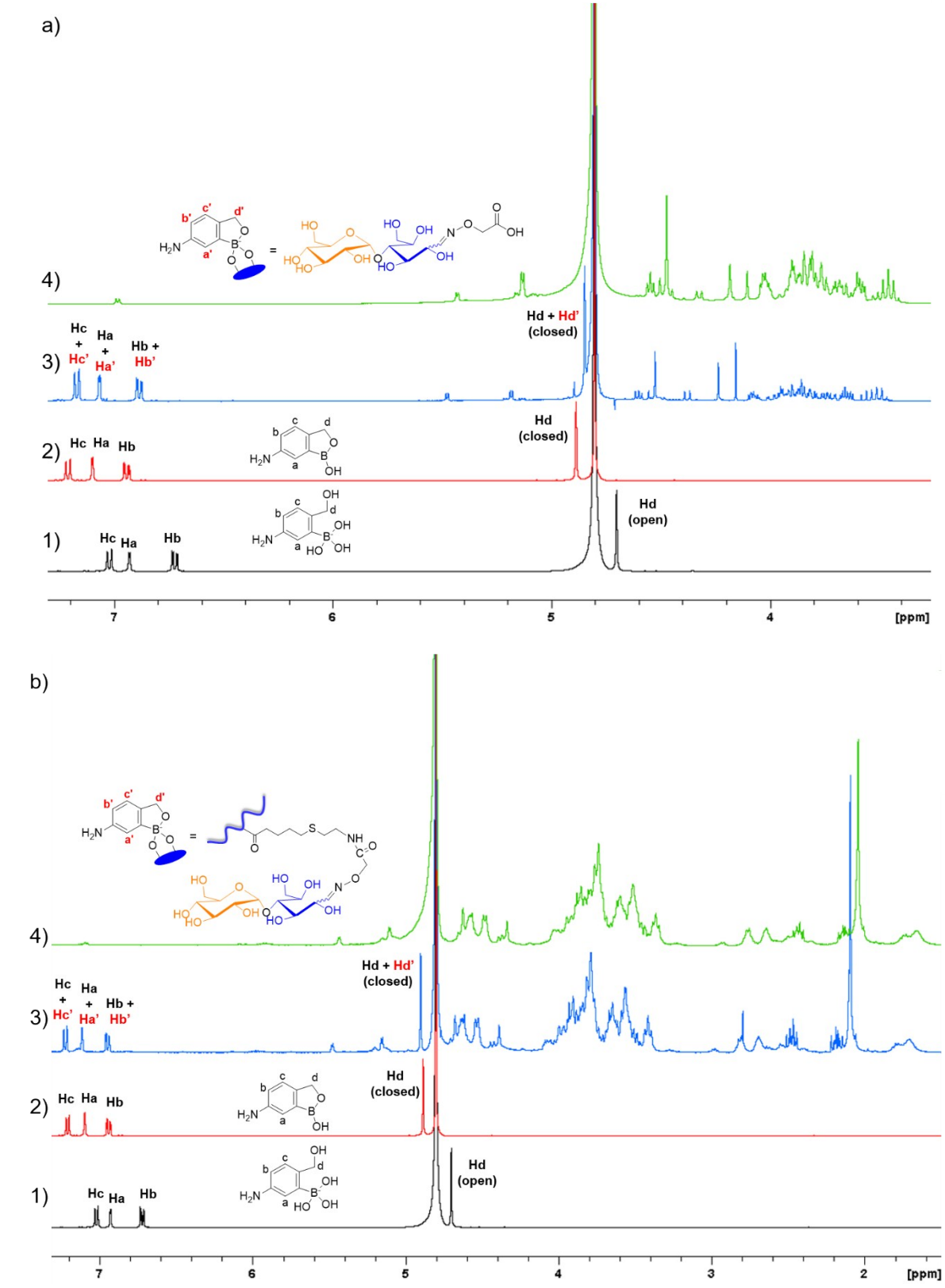

Figure S39. (a) ^{1}H NMR spectra of ABOR alone at pD 11-12 (1), at pD 7.4 (2), ABOR in the presence of maltose-COOH (3) at pD 7.4 and maltose-COOH alone (4). (b) ^{1}H NMR spectra of ABOR alone at pD 11-12 (1), at pD 7.4 (2), ABOR in the presence of HA-maltose (3) at pD 7.4 and HA-maltose alone (4) (ABOR/maltose molar ratio of 1:1).

31. Evidence of the partial opening of the endocyclic B-O bond of ABOR bound to free/grafted gluconamide by ^{1}H NMR spectroscopy

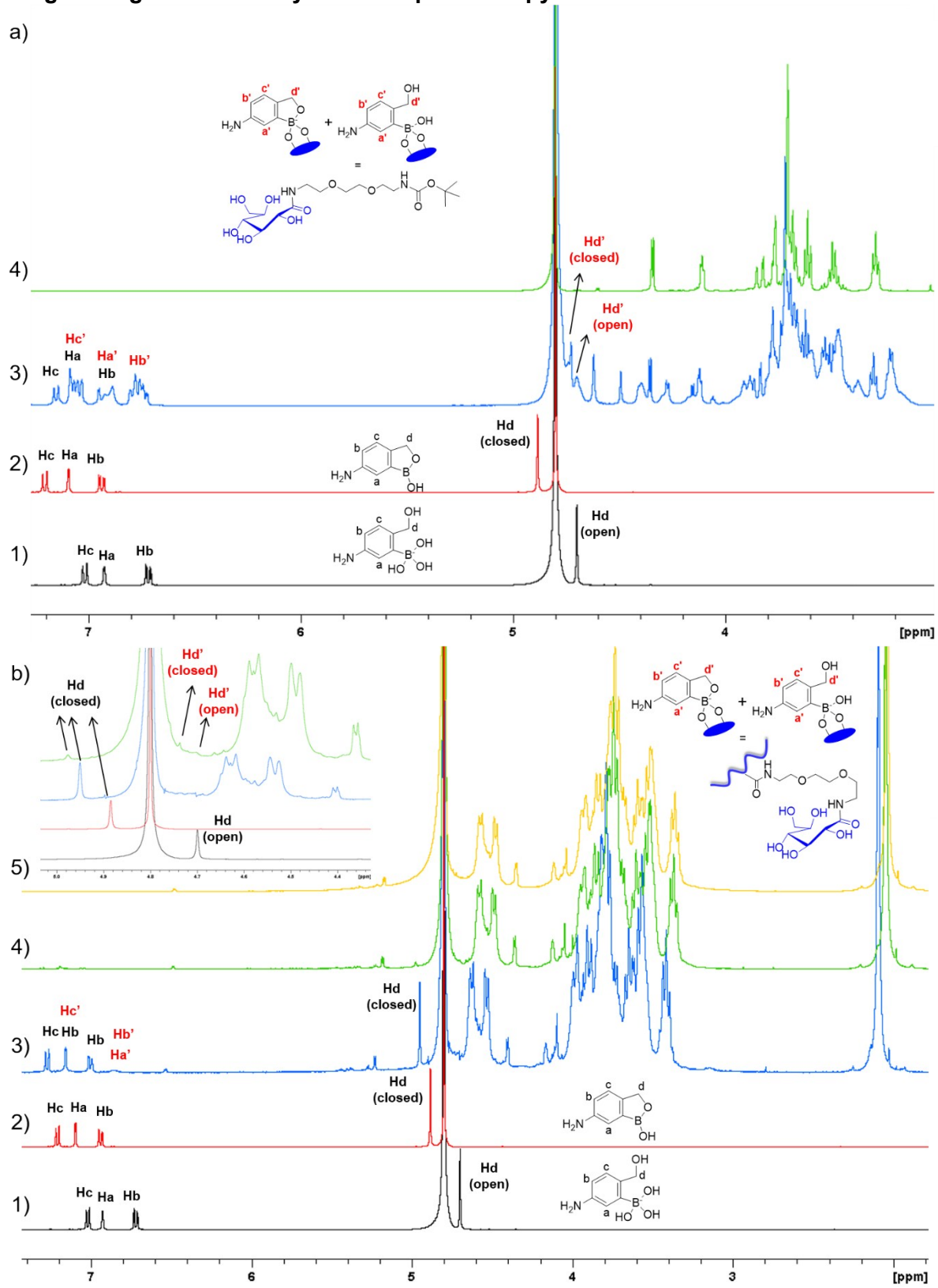

Figure S40. (a) ^{1}H NMR spectra of ABOR alone at pD 11-12 (1), at pD 7.4 (2), ABOR in the presence of free gluconamide (3) at pD 7.4 and free gluconamide alone (4). (b) ^{1}H NMR spectra of ABOR alone at pD 11-12 (1), at pD 7.4 (2), ABOR in the presence of HA-gluconamide (3 and 4, ABOR/gluconamide molar ratios of 1:1 and 1:10, respectively) at pD 7.4 and HA-gluconamide alone (5).

32. Dynamic rheological analysis of HA-PBA/HA-catecholamine (dopamine) at pH 7.4

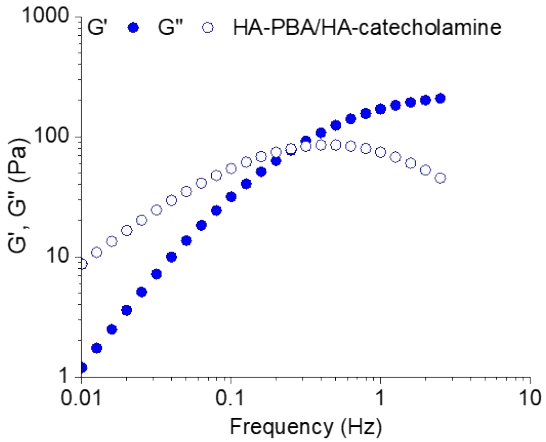

Figure S41. Frequency dependence of G' and G" showing the fast network relaxation of a mixture of HA-PBA with a HA-catecholamine conjugate.

33. Mechanism of boronate ester formation

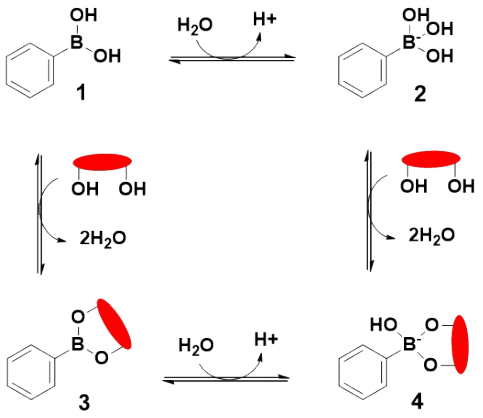

Figure S42. Equilibria between phenylboronic acid and diol-containing molecules in aqueous solution.[29] It is traditionally believed that boronate esters are mainly formed via the boronate anion (2). Recent studies, however, have shown that the kinetically preferred pathway to the boronate ester species is via the trigonal boronic acid (1).[30,31] This includes formation of a neutral diester (3) by reaction of 1 and the diol-containing molecule, which reacts with a water molecule in a second step to produce the anionic tetrahedral diester adduct (4).

34. References

(1) Macosko, C. W. G. *Rheology: Principles, Measurements, and Applications*; VCH Publishers: Weinheim, Germany, **1994**.

(2) Krieger, I. M. Bingham Award Lecture—1989: The Role of Instrument Inertia in Controlled-stress Rheometers. *J. Rheol.* **1990**, *34* (4), 471–483.

(3) Hudson, R. E.; Holder, A. J.; Hawkins, K. M.; Williams, P. R.; Curtis, D. J. An Enhanced Rheometer Inertia Correction Procedure (*ERIC*) for the Study of Gelling Systems Using Combined Motor-Transducer Rheometers. *Phys. Fluids* **2017**, *29* (12), 121602.

(4) Abraham, M. J.; Murtola, T.; Schulz, R.; Páll, S.; Smith, J. C.; Hess, B.; Lindahl, E. GROMACS: High Performance Molecular Simulations through Multi-Level Parallelism from Laptops to Supercomputers. *SoftwareX* **2015**, *1–2*, 19–25.

(5) Berendsen, H. J. C.; Postma, J. P. M.; van Gunsteren, W. F.; Hermans, J. Interaction Models for Water in Relation to Protein Hydration. In *Intermolecular Forces*; Springer: Dordrecht, 1981; pp 331–342.

(6) Schmid, N.; Eichenberger, A. P.; Choutko, A.; Riniker, S.; Winger, M.; Mark, A. E.; van Gunsteren, W. F. Definition and Testing of the GROMOS Force-Field Versions 54A7 and 54B7. *Eur. Biophys. J.* **2011**, *40* (7), 843–856.

(7) Bussi, G.; Donadio, D.; Parrinello, M. Canonical Sampling through Velocity Rescaling. *J. Chem. Phys.* **2007**, *126* (1), 014101.

(8) Berendsen, H. J. C.; Postma, J. P. M.; van Gunsteren, W. F.; DiNola, A.; Haak, J. R. Molecular Dynamics with Coupling to an External Bath. *J. Chem. Phys.* **1984**, *81* (8), 3684–3690.

(9) Frisch, M. J.; Trucks, G. W.; Schlegel, H. B.; Scuseria, G. E.; Robb, M. A.; Cheeseman, J. R.; Scalmani, G.; Barone, V.; Mennucci, B.; Petersson, G. A.; Nakatsuji, H.; Caricato, M.; Li, X.; Hratchian, H. P.; Izmaylov, A. F.; Bloino, J.; Zheng, G.; Sonnenberg, J. L.; Hada, M.; Ehara, M.; Toyota, K.; Fukuda, R.; Hasegawa, J.; Ishida, M.; Nakajima, T.; Honda, Y.; Kitao, O.; Nakai, H.; Vreven, T.; Montgomery, J., J. A.; Peralta, J. E.; Ogliaro, F.; Bearpark, M.; Heyd, J. J.; Brothers, E.; Kudin, K. N.; Staroverov, V. N.; Kobayashi, R.; Normand, J.; Raghavachari, K.; Rendell, A.; Burant, J. C.; Iyengar, S. S.; Tomasi, J.; Cossi, M.; Rega, N.; Millam, J. M.; Klene, M.; Knox, J. E.; Cross, J. B.; Bakken, V.; Adamo, C.; Jaramillo, J.; Gomperts, R.; Stratmann, R. E.; Yazyev, O.; Austin, A. J.; Cammi, R.; Pomelli, C.; Ochterski, J. W.; Martin, R. L.; Morokuma, K.; Zakrzewski, V. G.; Voth, G. A.; Salvador, P.; Dannenberg, J. J.; Dapprich, S.; Daniels, A. D.; Farkas, Ö.; Foresman, J. B.; Ortiz, J. V.; Cioslowski, J.; Fox, D. J. *Gaussian 09, Revision D.01*; Gaussian, Inc.: Wallingford CT., 2009.

(10) Zhao, Y.; Truhlar, D. G. The M06 Suite of Density Functionals for Main Group Thermochemistry, Thermochemical Kinetics, Noncovalent Interactions, Excited States, and Transition Elements: Two New Functionals and Systematic Testing of Four M06-Class Functionals and 12 Other Functionals. *Theor. Chem. Acc.* **2008**, *120* (1), 215–241.

(11) Marenich, A. V.; Cramer, C. J.; Truhlar, D. G. Universal Solvation Model Based on Solute Electron Density and on a Continuum Model of the Solvent Defined by the Bulk Dielectric Constant and Atomic Surface Tensions. *J. Phys. Chem. B* **2009**, *113* (18), 6378–6396.

(12) Del Vigo, E. A.; Marino, C.; Stortz, C. A. Exhaustive Rotamer Search of the 4C1 Conformation of α- and β-d-Galactopyranose. *Carbohydr. Res.* **2017**, *448*, 136–147.

(13) Sameera, W. M. C.; Pantazis, D. A. A Hierarchy of Methods for the Energetically Accurate Modeling of Isomerism in Monosaccharides. *J. Chem. Theory Comput.* **2012**, *8* (8), 2630–2645.

(14) Mierzwa, G.; Gordon, A. J.; Latajka, Z.; Berski, S. On the Multiple BO Bonding Using the Topological Analysis of Electron Localisation Function (ELF). *Comput. Theor. Chem.* **2015**, *1053*, 130–141.

(15) Mergy, J.; Fournier, A.; Hachet, E.; Auzély-Velty, R. Modification of Polysaccharides via Thiol-Ene Chemistry: A Versatile Route to Functional Biomaterials. *J. Polym. Sci. Part Polym. Chem.* **2012**, *50* (19), 4019–4028.

(16) Tarus, D.; Hachet, E.; Messager, L.; Catargi, B.; Ravaine, V.; Auzély-Velty, R. Readily Prepared Dynamic Hydrogels by Combining Phenyl Boronic Acid- and Maltose-Modified Anionic Polysaccharides at Neutral PH. *Macromol. Rapid Commun.* **2014**, *35* (24), 2089–2095.

(17) D'Este, M.; Eglin, D.; Alini, M. A Systematic Analysis of DMTMM vs EDC/NHS for Ligation of Amines to Hyaluronan in Water. *Carbohydr. Polym.* **2014**, *108*, 239–246.

(18) Auzély-Velty, R.; Rinaudo, M. New Supramolecular Assemblies of a Cyclodextrin-Grafted Chitosan through Specific Complexation. *Macromolecules* **2002**, *35* (21), 7955–7962.

(19) Cayot, P.; Tainturier, G. The Quantification of Protein Amino Groups by the Trinitrobenzenesulfonic Acid Method: A Reexamination. *Anal. Biochem.* **1997**, *249* (2), 184–200.

(20) Hermanson, G. Bioconjugate Techniques - 3rd Edition. In *Bioconjugate Techniques*; Academic Press: San Diego, California, 1996; pp 112–113.

(21) Ellis, G. A.; Palte, M. J.; Raines, R. T. Boronate-Mediated Biologic Delivery. *J. Am. Chem. Soc.* **2012**, *134* (8), 3631–3634.

(22) Dowlut, M.; Hall, D. G. An Improved Class of Sugar-Binding Boronic Acids, Soluble and Capable of Complexing Glycosides in Neutral Water. *J. Am. Chem. Soc.* **2006**, *128* (13), 4226–4227.

(23) Bérubé, M.; Dowlut, M.; Hall, D. G. Benzoboroxoles as Efficient Glycopyranoside-Binding Agents in Physiological Conditions: Structure and Selectivity of Complex Formation. *J. Org. Chem.* **2008**, *73* (17), 6471–6479.

(24) Cromwell, O. R.; Chung, J.; Guan, Z. Malleable and Self-Healing Covalent Polymer Networks through Tunable Dynamic Boronic Ester Bonds. *J. Am. Chem. Soc.* **2015**, *137* (20), 6492–6495.

(25) Inoue, Y.; Miyauchi, M.; Nakajima, H.; Takashima, Y.; Yamaguchi, H.; Harada, A. Self-Threading and Dethreading Dynamics of Poly(Ethylene Glycol)-Substituted Cyclodextrins with Different Chain Lengths. *Macromolecules* **2007**, *40* (9), 3256–3262.

(26) Thordarson, P. Determining Association Constants from Titration Experiments in Supramolecular Chemistry. *Chem Soc Rev* **2011**, *40* (3), 1305–1323.

(27) Sandström, J. *Dynamic NMR Spectroscopy*, Academic Press: London, **1982**; Vol. 86.

(28) Sutherland, I. *O. Annu. Rep. NMR (Nucl. Magn. Resonance) Spectrosc.* **1971**, *4*, 71–235.

(29) Springsteen, G.; Wang, B. A Detailed Examination of Boronic Acid–Diol Complexation. *Tetrahedron* **2002**, *58* (26), 5291–5300.

(30) Miyamoto, C.; Suzuki, K.; Iwatsuki, S.; Inamo, M.; Takagi, H. D.; Ishihara, K. Kinetic Evidence for High Reactivity of 3-Nitrophenylboronic Acid Compared to Its Conjugate Boronate Ion in Reactions with Ethylene and Propylene Glycols. *Inorg. Chem.* **2008**, *47* (5), 1417–1419.

(31) Peters, J. A. Interactions between Boric Acid Derivatives and Saccharides in Aqueous Media: Structures and Stabilities of Resulting Esters. *Coord. Chem. Rev.* **2014**, *268*, 1–22.